Masters Program in **Geospatial Technologies**

Dissertation submitted in partial fulfilment of the requirements for the Degree of *Master of Science in Geospatial Technologies*

PREDICTIVE MODELLING OF BUILT-UP SETTLEMENT EXPANSION IN THE WEST BANK USING MACHINE LEARNING AND CA-MARKOV METHODS

Nolan Richard Kressin

NOVA IMS INFORMATION MANAGEMENT SCHOOL
UNIVERSITAT JAUME·I
Universität Münster

NOVA Information Management School

Instituto Superior de Estatística e Gestão de Informação

Universidade Nova de Lisboa

PREDICTIVE MODELLING OF BUILT-UP SETTLEMENT EXPANSION IN THE WEST BANK USING MACHINE LEARNING AND CA-MARKOV METHODS

by

Nolan Richard Kressin

Master Dissertation presented as partial requirement for obtaining the Master's Degree in Geospatial Technologies

Supervised by

Hugo Alexandre Gomes da Costa, NOVA Information Management School

Ana Cristina Costa, NOVA Information Management School

Jorge Mateu, Universitat Jaume I

February, 2026

STATEMENT OF INTEGRITY

I declare that the work described in this document is my own and not from someone else. All the assistance I have received from other people is duly acknowledged and all the sources (published or not published) are referenced.

This work has not been previously evaluated or submitted to NOVA Information Management School or elsewhere. I further declare that I have fully acknowledged the Rules of Conduct and Code of Honor from the NOVA Information Management School.

Lisboa, February 24th, 2026

Nolan Richard Kressin

Recoverable Signature

X Nolan Kressin

Nolan Kressin

Signed by: c66510fc-9e6d-4588-ad26-8a82411fd24f

USE OF GENERATIVE ARTIFICIAL INTELLIGENCE

Tasks	NO	YES	Generative Artificial Intelligence tools
Better understand issues related to the research		x	ChatGPT, Gemini
Summarizing text from bibliography / resources		x	NotebookLLM
Summarizing the method(s) used		x	ChatGPT, Gemini, NotebookLLM
Translating text	x		
Grammar check		x	ChatGPT
Paraphrase or rewriting text from other people / resources	x		
Coding in R, Python, etc.		x	ChatGPT, Gemini, Claude
Get help on a software		x	ChatGPT, Gemini
Creating and editing images, maps, videos, etc.	x		

Data analysis	x		
Specify below other tasks not mentioned above:			

ACKNOWLEDGMENTS

I would like to thank all who assisted me during this thesis and master's program. First, all my lovely classmates (and roommates!) who I am so grateful for their company and friendship.

Secondly, my supervisors, for taking the time to review my very messy work and having endless patience with me.

Third, thank you to Dr. Ahmed Ghodieh for giving me some important datasets that I would not have been able to perform this thesis without!

Finally, thank you to my family; my dad and mom and sisters for their support.

PREDICTIVE MODELLING OF BUILT-UP SETTLEMENT EXPANSION IN THE WEST BANK USING MACHINE LEARNING AND CA-MARKOV METHODS

ABSTRACT

This thesis investigates the built-up expansion of Israeli settlements in the contested West Bank using multi-temporal satellite imagery, random forest (RF) modelling, and machine-learning (ML) assisted CA-Markov (Cellular Automata) modelling with TerrSet Land Change Modeler (LCM). The research aims to quantify historical land use and land cover (LULC) changes in the West Bank between 1994, 2014, and 2024 and to predict future urban settlement growth for 2034 and 2054. Utilizing Landsat-5 and Landsat 8-9 imagery at 30-meter resolution, the study employs a supervised RF algorithm to classify LULC and analyze settlement urban expansion. We reveal a significant transformation of the study area, with settlements more than doubling in area over the thirty-year study period, primarily at the expense of agricultural and bare land. To predict future growth, the research utilizes a ML-assisted CA-Markov model within the LCM framework. Three policy-driven scenarios: Business-as-Usual (BAU), Low-growth/High-constraint, and High-growth/Low-constraint, are simulated to predict future urban settlement growth for 2034 and 2054. We identify proximity to existing 1994 settlement footprints and road networks as the most influential drivers of growth. Validation of the predictive model against actual 2024 data illustrated moderate agreement, with a Figure of Merit of 22.05%, highlighting challenges in accurately allocating change in a volatile environment. We find that historical settlement growth was more concentrated near the Jerusalem metropolitan area, while future projections suggest a more dispersed pattern across the study region. By bridging remote sensing methodology with the analysis of politically contested land transitions, this thesis provides a novel, automated framework for monitoring settlement expansion in data-scarce and politically volatile areas. These findings offer valuable insights for regional planning and provide a transparent, reproducible method for documenting spatial transitions in conflict-affected, data-scarce landscapes.

KEYWORDS

Remote Sensing; Urban Growth Modelling; Random Forest; CA-Markov; West Bank; Israeli Settlements

Sustainable Development Goals (SGD):

INDEX

Table of Contents

INDEX OF TABLES

INDEX OF FIGURES

ACRONYMS

ANN: Artificial Neural Network or Multi-layer Perceptron

AHP: Analytical Hierarchical Processing.

AOI: Area of Interest.

BAU: Business-as-Usual.

CA-MARKOV: Cellular Automata – Markov.

CARTs: Classification and Regression Trees.

CAGR: Compound Annual Growth Rate.

CSRS: Coordinate Reference System.

CV: Coefficient of variation.

DBSI: Dry Bare-Soil Index.

DF: DecisionForest.

DTW: Dynamic Time Warping.

ER: Explanatory Ratio.

EVI: Enhanced Vegetation Index.

FoM: Figure of Merit.

GEE: Google Earth Engine.

GLC-FCS30D: Global Land Cover Fine Classification System at 30 m.

HMM: Hidden Markov Model.

ISP: Israeli settlement policy.

KDE: Kernel Density Estimation.

Klocation: Kappa for Location.

KNo: Kappa for No Information.

KStandard: Kappa Standard.

LCM: Land Change Modeler.

LULC: Land Use – Land Cover.

LR: Literature Review.

ML: Machine Learning.

MLP: Multi-Layer Perceptron.

MNDBI: Modified Normalized Difference Built-up Index.

MNDWI: Modified Normalized Difference Water Index.

MOLUSCE: Modules for Land Use Change Evaluation.

MSLC: Maximum Likelihood Classifier

NBR: Normalized Burn Ratio.

NDMI: Normalized Difference Moisture Index.

NDVI: Normalized Difference Vegetation Index.

NIR: Near Infrared.

OA: Overall Accuracy.

OOB: Out-of-Bag.

Px: Pixel.

RF: Random Forest.

RS: Remote Sensing.

SAVI: Soil-Adjusted Vegetation Index.

SWIR: Short-Wavelength Infrared.

SVM: Support vector machines.

UNHRC: United Nations Human Rights Council.

UTM: Universal Transverse Mercator.

WNL: Weighted Normalized Likelihood.

1 INTRODUCTION

The West Bank, Palestine has witnessed ongoing disputes over land, governance, and sovereignty, and remains a prudent example of an ongoing human rights crisis occurring in the modern world (Abbas et al., 2024). International organizations have raised alarms in the West Bank about the humanitarian implications of settlement expansion, military incursions, and the lack of infrastructure in Palestinian-administered areas (Allegra & Maggor, 2022). Most significant to the crisis has been Israel's unlawful urban settlement policy in the West Bank, which since the 1960s, has displaced millions of Palestinian peoples and is now home to over 700,000 settlers (Tenenbaum & Eiran, 2005; United Nations, 2023).

Remote sensing technologies have emerged as critical tools in evaluating these humanitarian situations. Satellite imagery and geospatial analysis enable objective, scalable assessments of land use, urban expansion, and environmental degradation (Ghodieh, 2020). Machine-learning (ML) techniques, such as Random Forest (RF), and CA-Markov (Cellular Automata - Markov) modelling, have emerged as strong tools for illustrating complex urban growth dynamics in data scarce environments (Asif et al., 2023; Attaallah, 2018; Duan et al., 2025; Tang et al., 2024). Understanding how these urban settlements will expand over time and impact land-use and land-cover (LULC) in the West Bank is of utmost importance for human-rights based organizations, especially those concerned with the ongoing displacement of the Palestinian peoples.

Although there is a plethora of research existing on the various impacts of urban growth to the Palestinian people, there still lacks systematic, long-term, and automated modelling of urban settlement change and LULC impact in the West Bank. Most existing studies focus on shorter timeframes (Ghodieh, 2020), broader overviews of the situation (Helu, 2012; Moghayer et al., 2017; Zerbini & Fradley, 2018), or have not focused their scopes on Israeli settlements specifically in the West Bank (Abuelaish & Olmedo, 2016; Attaallah, 2018; Holail et al., 2024; Kuhail & Radwan, 2025).

This thesis seeks to fill that gap by applying automated machine learning methods to quantify LULC changes in selected Israeli settlements in historical dates, then applying the CA-Markov model to predict urban growth and impact on LULC.

2 LITERATURE REVIEW

The purpose of the literature review (LR) is to present the necessary background used throughout this thesis and bridge gaps in multidisciplinary knowledge. The LR is structured in two main sections: the history of the conflict as well as the current reality on the ground, then thirdly urban growth modelling, where we present the current research in the area and identify research gaps.

2.1 West Bank Settlements And Human Rights

2.1.1 General Overview

The political issue of Israeli settlements encompasses a long, complex history, and witnesses the intersection of geopolitical interests, religious ideology, and varied economic and social needs of the Israeli people. Summarizing these problems into a concise LR is not wholly sufficient, however within the scope of urban growth prediction, we can better focus our research.

The United Nations Human Rights Council (UNHRC), in its 2013 fact finding mission report, defines settlements as ‘all physical and non-physical structures and processes that constitute, enable and support the establishment, expansion and maintenance of Israeli residential communities beyond the Green Line of 1949 in the Occupied Palestinian Territory’ (UNHRC, 2013). The Green Line of 1949 refers to line of armistice drawn between Israel and its neighbours of Syria, Egypt, Lebanon, and Jordan after their war for independence (UNTERM, 2013). The UN also accounts for ‘outposts’, which are another frequent term used discussing settlements. Outposts are settlements not formally recognised by the Israeli government – although all the settlements are illegal in an international context anyways (UNHRC, 2013; UNRWA, 2025). Further, settlements need not be necessarily formally built by Israeli forces. Many settlements have been occupied from displaced Palestinians (Muhsen, 2017; Schwake, 2020).

We have defined settlements physically, such as through built-up infrastructure, buildings, and roads, but the UN definition also refers to the ‘non-physical structures.’ As Ghodieh states in his 2020 paper, Israeli settlements reach far beyond their visible, physical boundaries – the impact of occupation is felt everywhere in Palestinian lives (Ghodieh, 2020). It is imperative to note that these impacts are felt not just in areas adjacent to the settlements, but in life in occupied Palestine as a whole.

Currently, the United Nations estimates that there are over 700,000 Israeli settlers, of which 503,732 live in the West Bank, and 233,600 in East Jerusalem (UNRWA, 2025). This population is spread across 147 settlements and 224 outposts throughout the West Bank and East Jerusalem (Figure 2-1). These settlements have been placed in Area ‘C’ – which are administrative areas of land of differentiating governmental control defined by the Oslo accords of 1995. Area ‘A’, about 18% of the region, is controlled fully by the Palestinian Authority (PA). Area ‘B’, comprised of 22% of the West Bank, is under Palestinian civic control but joint Palestinian/Israeli security control. Finally, Area ‘C’, comprising most of the West Bank, is fully controlled by the Israeli government.

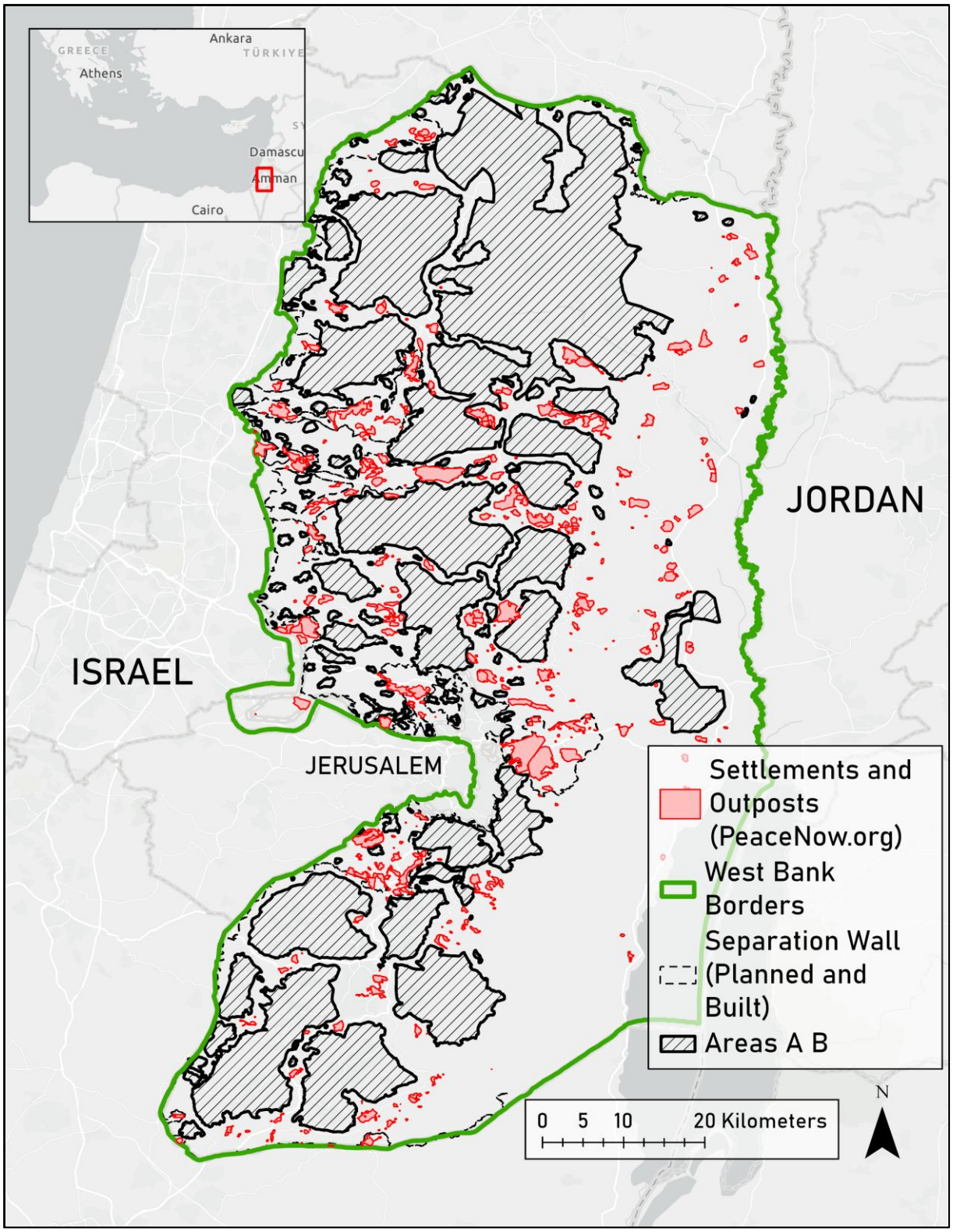

Figure 2-1. Borders of the West Bank. To the west is Israel, and east of Jordan. Red areas are settlement extent polygons generated by PeaceNow.org. Area C would be the area within the West Bank borders not represented by Areas A B in this map.

Settlements have been actively supported by the Israeli government, who have directed planning, construction, development, consolidation, and incentivization of settlement colonization through direct policy instruments (UNHRC, 2013). These policy instruments include the building of infrastructure for settlements, advertisement and financial incentives to move for Jewish people within Israel, sponsorship of economic activities, delivery of public service and development projects within settlements, and finally the formal seizure of Palestinian land for military and public 'needs', or for the designation as State land.

To fully understand the role and motivations of the Israeli government, the historical context of their decisions is also required.

2.1.2 History of Israeli Settlement Policy

Much of this section takes inspiration from the work of Tenenbaum and Eiran, who in their 2005 paper on the brief history of settlement in the West Bank, outline the stages of Israeli settlement policy (ISP) from after the Six-Day-War to the early 21st century.

Although Jewish settlement in historic Palestine dates to the late 19th and early 20th centuries alongside the rise of Zionism, most scholarship identifies the contemporary settlement project in the West Bank as beginning after the 1967 Six-Day War, when Israel captured the territory from Jordan (Allegra & Maggor, 2022; Muhsen, 2017). Initially, the West Bank was viewed more as a strategic bargaining chip than a site for civilian expansion, with proposals to exchange occupied land for peace agreements (Tenenbaum & Eiran, 2005). At the same time, figures such as Yigal Alon advanced plans to establish settlements along the Jordan Valley as defensive buffers, deliberately locating them outside densely populated Palestinian areas while envisioning possible future annexation.

From the mid-1970s onward, settlement activity became increasingly ideological and state supported (Helu, 2012). The rise of Gush Emunim and later Likud governments accelerated expansion, framing settlements as instruments of security, territorial consolidation, and Zionist fulfillment (Tenenbaum & Eiran, 2005). Financial incentives

and institutional backing from organizations such as the World Zionist Organization and the Jewish Agency transformed settlement from a limited strategic initiative into a sustained state-sponsored project (Tenenbaum & Eiran, 2005). The settler population grew rapidly through the 1980s and 1990s, despite the 2005 Disengagement Plan that removed settlements from Gaza while consolidating those in the West Bank (Spyer, 2006). Since then, Israeli policy has largely focused on strengthening and integrating West Bank settlements, reinforcing their status as a long-term and central feature of Israeli territorial strategy.

2.1.3 Modern Reality: Conflict and Legality

Currently, the Netanyahu government has dramatically increased settlement expansion. In the last 7 years, plans for settlement development have increased by 250%, from 11, 513 units in 2018 to 28,872 units in 2024 (UNRWA, 2025). The total number of settlement plans hit its total peak in 2023 at over 30,000, implicating the intentions of the current regime to continually settle and annex the West Bank in the future (UNRWA, 2025). Further, the nature of settlement expansion is also changing from vertical expansion to horizontal: in East Jerusalem, nearly half of all current settlement plans are for new territorial expansion (UNRWA, 2025). Israeli outposts have also been targeted by the government, with new policy instruments, such as the ‘bypass legalization mechanism’ easing the transition of outposts to formal, legalized settlements. This policy allowed for five outposts to be formalized as settlements in 2024. Settlements are being planned in a way of further fragmenting and obstructing Palestinian access to their lands, and development permits are also being accepted at diverging rates, with Palestinian permits being accepted at a far lower rate of 18%, and Israeli permits at over 30%.

The rapid expansion of Israeli settlements has also led to a dramatic increase in conflict between settlers and the Palestinian population. In 2024, 1,420 acts of violence were reported, a 32.5% increase from 2023, which was already the previous highest amount since violent incidents were recorded in 2026. Displacement is also a severe risk facing Palestinians; 47 communities have been forcibly displaced since 2023, and 50% of the 195 Palestinian communities in Area C of the West Bank are at an extreme risk of displacement. In refugee camps, 33,000 have been displaced,

most particularly in the Jenin, Nur Sham, and Tulkam refugee camps. More than 1000 home have been destroyed in various military operations within the West Bank, with additional thousands more damaged (UNHRC, 2025). Violence is everywhere in the West Bank and humanitarian action is required for Palestinian lives.

2.1.4 Drivers of Future Settlement Growth

The expansion of illegal settlements in the West Bank can be linked to two powerful, interlinked agents: the political will of the Israeli government and economic demands of their citizens (Allegra & Maggor, 2022). Firstly, there is demand for the government to exert political dominance over the Palestinian community through continued territorial dominance. This would lead to an expansion in settlements along the peripheries of the West Bank, where the Israeli government has otherwise little 'soft' power. A further element of settlement expansion along the peripheries of the West Bank, as mentioned earlier, are buffer towns that may serve as security and military outposts along the borders of the West Bank, such as the original settlements built along Highway 67 near the Jordanian border. These settlements – as categorized by Allegra & Magra (2022) - grew through ideological, agricultural, and strategic modes.

However, much scholarly research has pivoted from framing settlement expansion as purely political – now framing expansion economically (Schwake, 2020). Many of the highly populated settlements, such as Ma'ale Adumim, Alfei, and Efrat, were approved in areas of high demand for housing, near the already congested East Jerusalem and Tel Aviv metropolitan area (Allegra & Maggor, 2022). Building and investing in settlements nearby major metropolitan areas instead of peripheries had several major advantages for the Israeli government: reducing the per capita cost of maintenance, increasing housing supply, and efficiently increasing broad, diverse public support to settlement efforts and their political legitimacy (Schwake, 2020). Many residents of these settlements do not identify themselves as settlers, but rather as people taking advantage of an economic opportunity (Kraft, 2009). About 80-85% of the settlement population in the West bank resides in near proximity to the Green Line - hence, for research on settlement expansion and growth, a focus on settlements near to the Green Line would be essential (Allegra & Maggor, 2022).

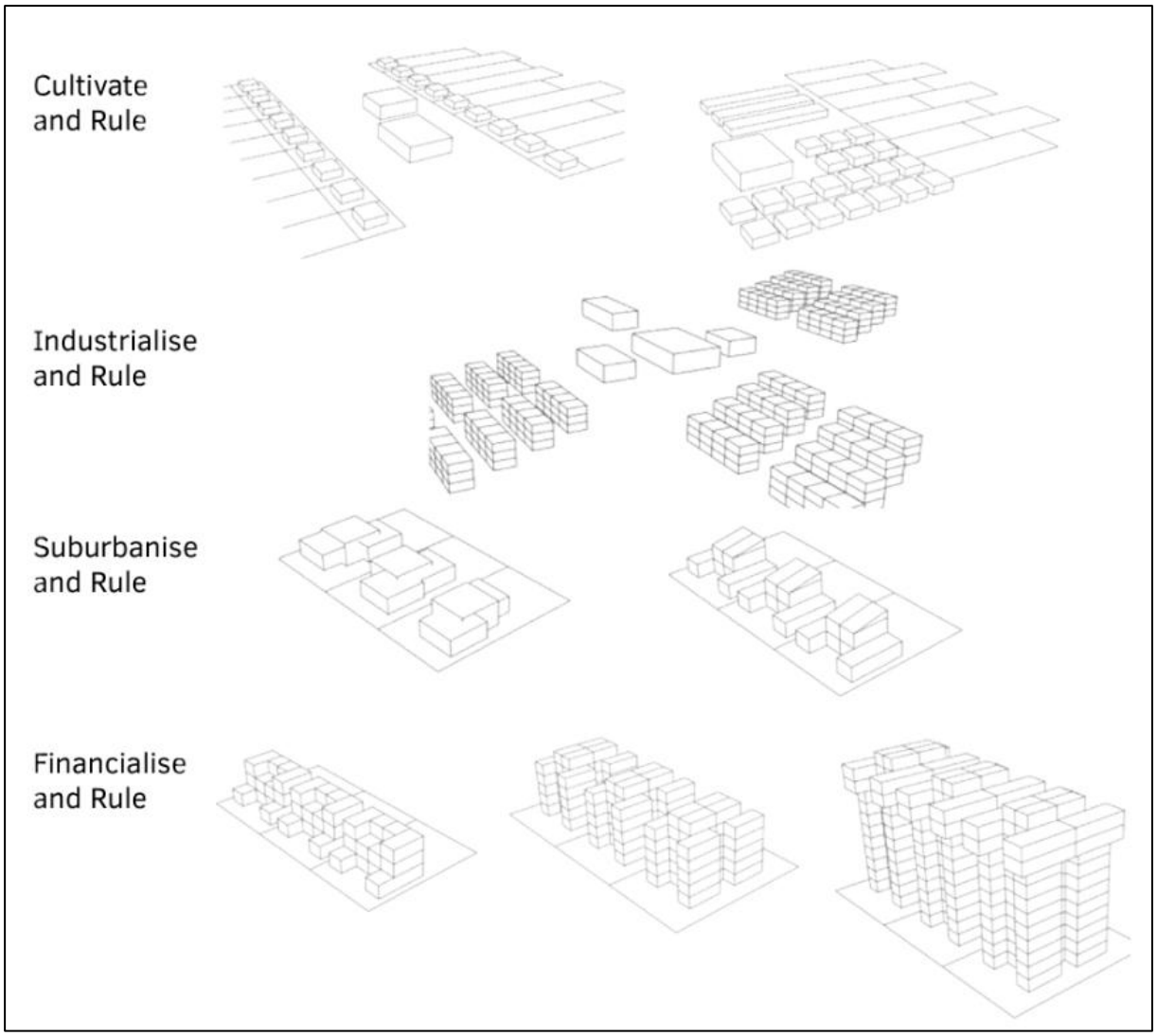

Figure 2-2. The four stages of historical Israeli settlement planning and development (Schwake, 2020).

2.2 URBAN GROWTH MODELLING REVIEW

Many methods exist to model and predict how built-up land, like in Israeli settlements, will expand in the future. In the scope of this dissertation, we will focus explicitly on spatial methods of urban built-up prediction.

To best capture trends in the current literature on urban growth prediction, a small LR was conducted on the Scopus platform to capture the most impactful, recent (>2019) research in the field. We used the prompt:

TITLE-ABS-KEY("urban built-up" OR "built-up expansion" OR "urban expansion" OR "urban growth" OR "urban sprawl") AND ("spatial model*" OR "spatial modelling" OR "urban growth model*" OR "change detection" OR prediction) AND ("remote sensing" OR "satellite imagery" OR Landsat OR Sentinel) AND ("arid" OR "dry" OR desert OR "semi-arid") AND PUBYEAR > 2019

This prompt resulted in 46 results, of which we included 15 papers. The prompt section ‘AND (arid OR dry OR desert OR "semi-arid”)’ was then removed, and the query ran again. 16 additional sources were added for analysis for a total of 31 papers. Exclusion criteria were that papers were not focused on urban growth modelling, were not peer-reviewed, or were in a foreign language. To assess how studies were monitoring and predicting LULC, we analysed each paper based on these prompts: does the study mention any satellites in their analysis, were any bands/indices mentioned in assessing LULC, what driving factors were identified to predict urban growth, what did the study use to model existing LUC, what did the study use to predict LULC in the future, what time-span did the study predict over, and how did the study assess the accuracy of their prediction(s)?

The LR is available in the Appendix A.

2.2.1 Literature Review Results

Most studies used Landsat 5,7,8, and 9 platforms in their assessment of urban LULC and prediction. Two studies opted to use other satellite platforms, those being Sentinel and SPOT (Al-Dousari et al., 2023; Boulila et al., 2021). Landsat was often cited due to its long temporal span (Khajuria & Kaushik, 2024; Nikoo et al., 2025), adequate spatial resolution (Nikoo et al., 2025; Singh et al., 2022), and cost-effectiveness (Abdelkarim, 2025; Dey et al., 2021). In terms of the bands used from the satellites, many papers do not explicitly mention the exact band or band indices, instead stating they used some form of false color composite (Dey et al., 2021; Falah et al., 2020; Vinayak et al., 2021). The band indices mentioned are most commonly the Normalized Difference Vegetation Index (NDVI) (Abdelkarim, 2025; Çağlıyan & Dağlı, 2022; Fattah et al., 2021; Yatoo et al., 2022), (Modified) Normalized Difference Water Index (MNDWI/NDWI) (Nikoo et al., 2025; Selmy et al., 2023), and the

(Modified) Normalized Difference Building Index (Ashwini & Sil, 2022; Çağlıyan & Dağlı, 2022).

Several important driving factors of urban growth were identified in the literature (Figure 2-3). Distance to roads is by far the most implemented driver, due to the accessibility of data for road networks (Yatoo et al., 2022) and its high predictive strength (Al-Dousari et al., 2023). Other highly popular variables included elevation and slope, distance to water bodies, and distance to cities/towns.

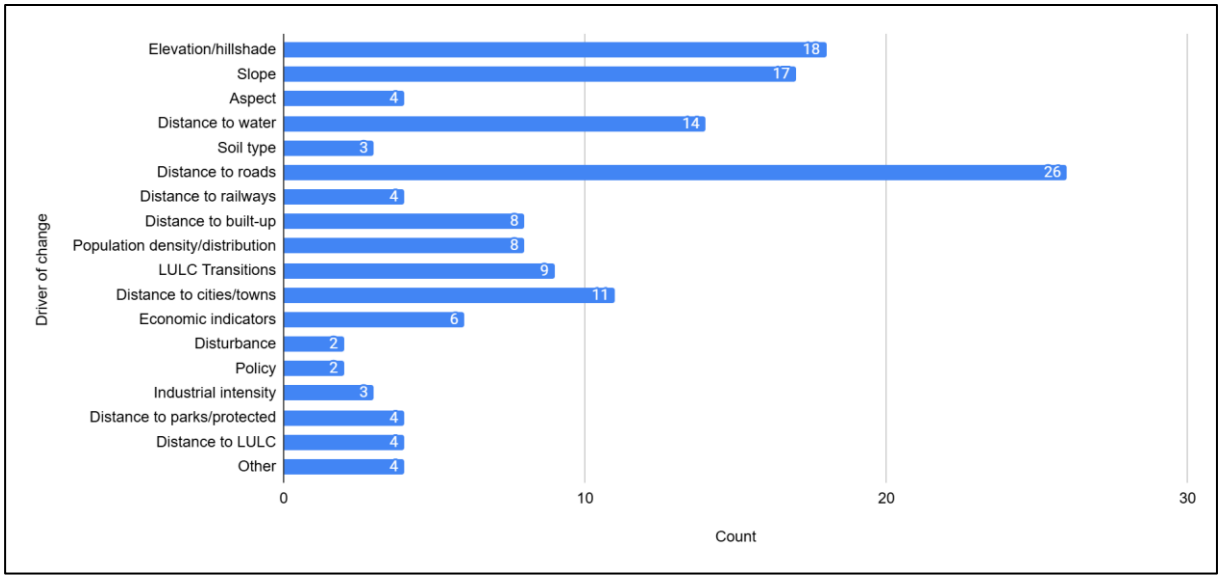

Figure 2-3. Drivers of LULC change mentioned in papers and count of number of times mentioned.

Two popular methods of modelling current LULC were identified: the Maximum Likelihood Classifier (MSLC) and RF (Figure 2-4). The MSLC was the most popular, being used in 14 papers, with RF behind it at 7 papers. Support vector machines (SVM), object-based classification, and DecisionTree classification methods were also mentioned more than once in the literature.

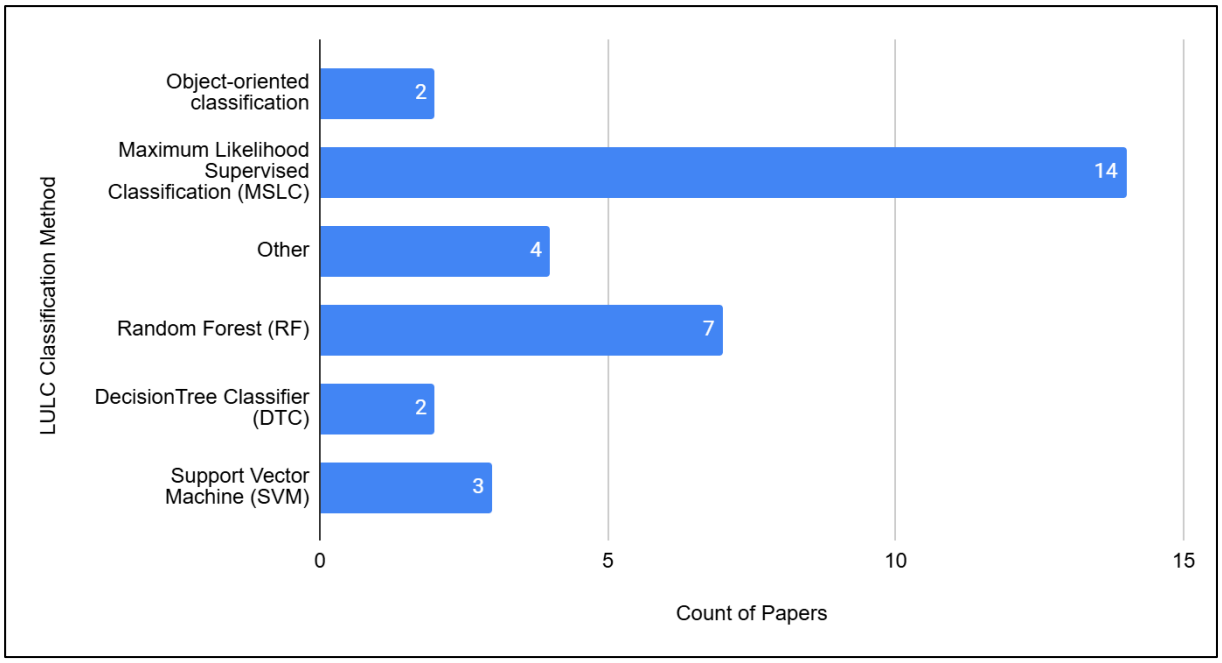

Figure 2-4. Classification methods of LULC used by papers and the number of times they were mentioned. One paper is double counted as it used both DecisionTree and RandomForest classifiers.

The most popular model for predicting future LULC was by far the LCM in TerrSet IDRISI software, being used in 9 papers (Figure 2-5). LCM was stated to be preferential due to its ability to model complex land dynamics at an instance (Alqadhi et al., 2021), proven effectiveness in other works (Abdelkarim, 2025), and ability to handle large amounts of data (Rimal et al., 2020). The next most preferred methods were CA-Markov, MOLUSCE, and AHP-CA.

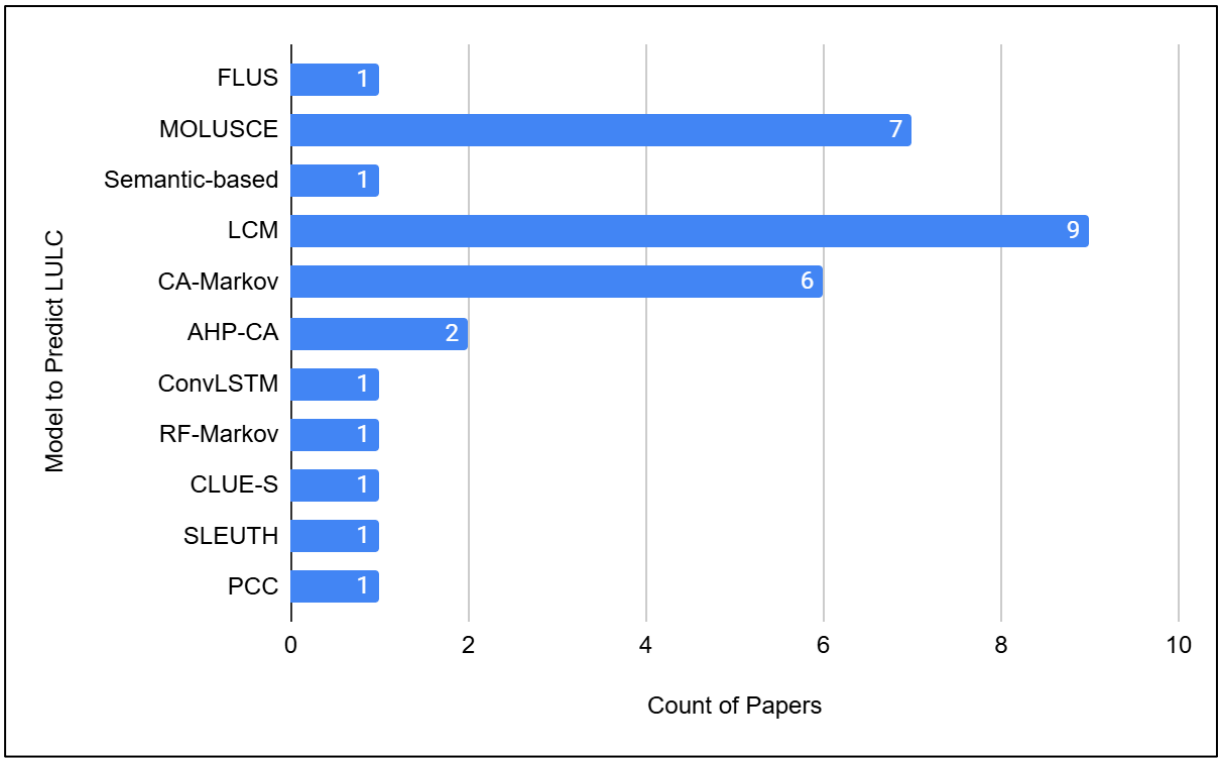

Figure 2-5. Models for predicting LULC used in papers and number of times mentioned.

Further, for predicting future LULC, the most common predictor years (by decade), years papers made predictions to (by decade), and number of time-steps used to make predictions were collected (Figure 2-6). Papers most used satellite images from the 2000s, 2010s, and 2020s to make predictions into the future, with 2020s being the most common. Most predictions were made for the 2030s. Finally, most papers used 4 time-steps to make future predictions (3 years for prediction, 1 for validation of prediction).

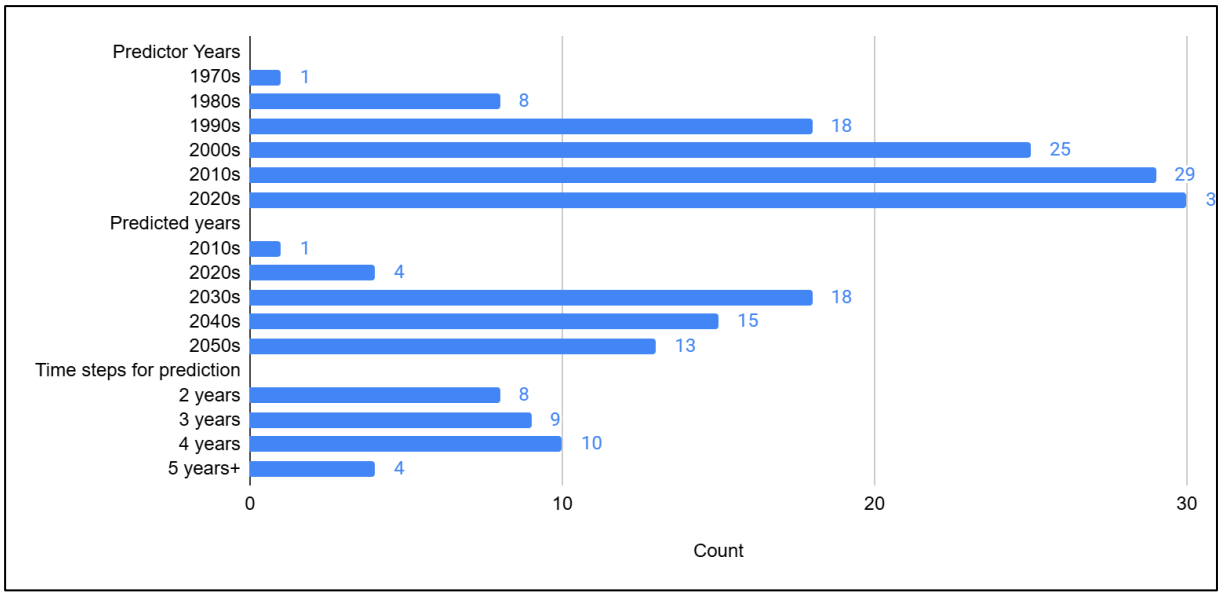

Figure 2-6. Years that papers use for prediction (by decade), years that papers predict to (by decade), and the number of time-steps paper use to make predictions.

Finally, the most common metrics for the accuracy of LULC predictions were evaluated (Figure 2-7). The overall accuracy (OA) was most reported, which is simply a comparison of how much the predicted image matches the reference image. When authors reported OA, they also commonly reported the Kappa coefficient to support their findings. Pontius Kappa metrics, such as Kappa for No Information (K_{No}), Kappa for Location ($K_{location}$), and Kappa Standard ($K_{Standard}$) are also somewhat commonly implemented but these were later discredited in one of Pontius' later papers (Pontius Jr & Millones, 2011; Pontius, 2002).

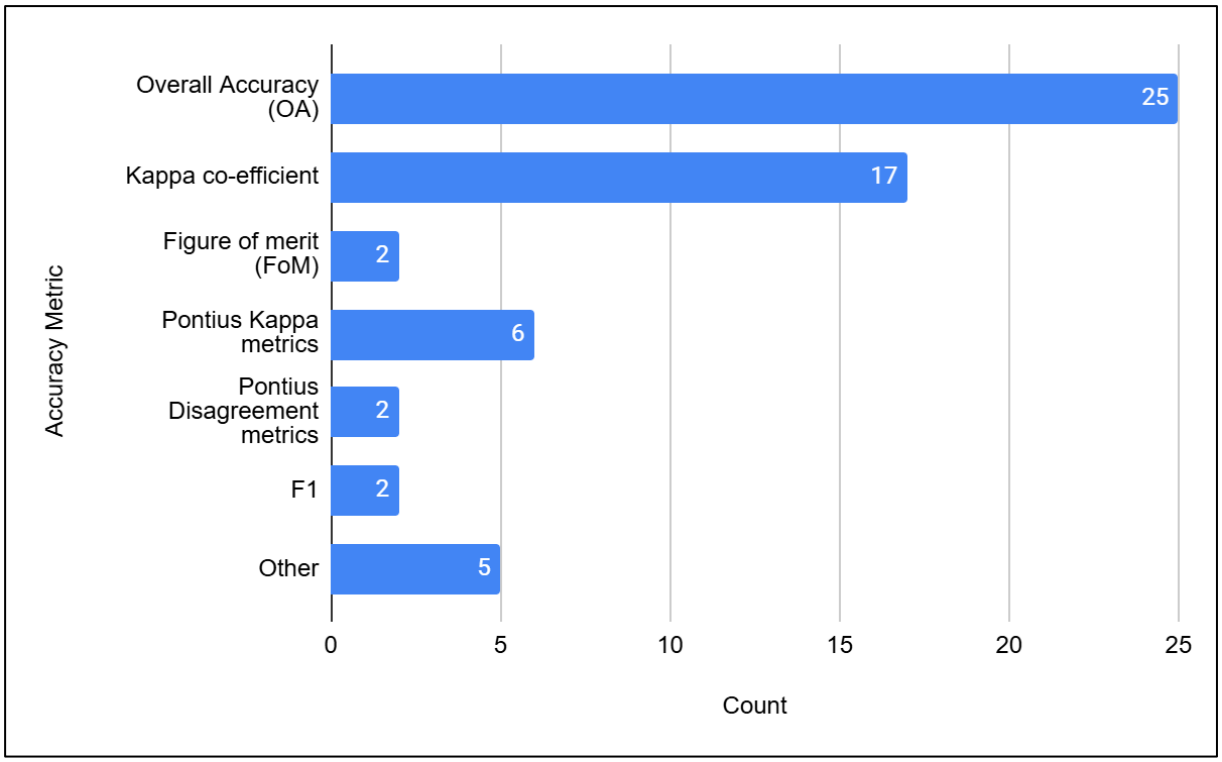

Figure 2-7. Accuracy metrics reported in the literature, and number of times they were implemented in all papers.

2.3 Research Gap

A further investigation using the same prompt was explored, but with the search terms “palestine” OR “gaza” OR “west bank” OR “israel”, and the exclusion of the “dry”/”semi-arid” search terms. The time restriction was also removed. This led to 6 results, none of which were relevant to the prediction of urban growth in settlements. Hence, the following research questions were proposed to fill in the research gap in settlement growth prediction.

2.4 Research Questions

1) How has the spatial extent and LULC of Israeli settlements and surrounding land in the West Bank changed between 1994, 2014, and 2024, as detected through multi-temporal satellite imagery and automated classification methods?

2) To what extent will Israeli settlements grow and change in the future, such as in 2034 and 2054 and according to scenarios of low-growth/high-constraints, business-as-usual (BAU), and high-growth/low-constraints?

3) Where will settlements expand the most in the study area, and within that expansion, what are the observable impacts on surrounding LULC classes?

3 METHODOLOGY

This section presents the methodology for classifying LULC and predicting future settlement growth in the study area. The methods are primarily inspired by the work of Badshah et al., 2024, and Tahir et al., 2025.

3.1 Study Area and Datasets

3.1.1 Area of Interest

The initial area of interest is the West Bank, a modern term denoting contested territory between Palestine and Israel (Figure 3-1). The West Bank is a politically complex location, split into three areas of political jurisdiction from the Oslo Agreement of 1995. Area 'C' composes roughly 61% of the territory and is under full control of the Israeli authority. Within this area are nearly all Israeli settlements, outposts, and militarily significant areas, and is home to 6-800,000 Israeli and Palestinian citizens (*Area C | B'Tselem*, 2024). Area 'A', about 18% of the West Bank, is controlled exclusively by the Palestinian authority. Area 'B', roughly 22% of the total West Bank, is under mixed control between both Palestinian and Israeli authorities, with Israeli governance controlling internal security affairs (Singer, 2021).

Topographically, the West Bank is split into four areas: the central highlands; the vast mountainous area between the cities of Jenin to Hebron, the semi-coastal zone of the north-west between Jenin and Tulkarm, the eastern slopes where the central highlands and desert of Jordan meet, and the Jordan Valley, a small strip of the Eastern slopes and Jordan river with high amounts of agricultural activity (Dudeen, 2013). The climates of the central and semi-coastal zones can be characterized as Mediterranean moderate climate, and these areas have generally higher population densities, increased agricultural activity, and denser vegetation cover than their eastern counterparts. In the east, the land has more bare soil and rocks, steeper elevation changes, and drier, hotter climatic conditions (Ghodieh, 2020). In this study,

most of the analysis occurs within the central highlands/Area ‘C’, as this is where most of the settlement population exist.

Within the West Bank, an initial set of ten settlements of interest were selected based on population size, according to census data from 2024 (Peace Now, 2025). Further, the chosen settlements must have been established before or on the initial date of analysis of 1994. More settlements which fell into the formal study area, described in section 3.1.2, were then added to the analysis (Table 1).

Table 1. Selected settlements and their founding dates, sorted by population count according to the most recent 2024 data (Peace Now, 2025). 35 total settlements were analysed.

Major Settlements:	**Founding Date**	**Population (May 2024)**
Modi'in Ilit	1994[1]	86,816
Beitar Illit	1985	68,293
Ma'ale Adumim	1975	38,097
Giva'at Ze'ev	1983	22,503
Ariel	1978	21,004
Efrata	1980	11,940
Karnei Shomron	1978	10,179
Oranit	1985	9,397
Alfei Menashe	1983	8,000
Kochav Ya'akov	1977	3,138
Settlements included:		
Sha'arei Tikva	1983	6,122
Geva Binyamin (aka Adam)	1984	6,115
Immanuel	1983	5,142
Elkana	1977	4,453
Alon Shvut	1970	2,967
Na'ale	1988	2,955
Ganei Modiin	1985	2,772
Yakir	1981	2,758
El'azar	1975	2,712
Tzofim	1989	2,700
Hashmonaim	1985	2,504
Neve Daniel	1982	2,383

[1] The founding date of Modi’in Illit appears slightly contested. The settlement was formally designated as a local council in 1996, but numerous sources state its founding as in 1994 or earlier (Kraft, 2009; *Modi’in Illit (West Bank)* | *The National Library of Israel*, n.d.; The Applied Research Institute – Jerusalem, 2008).

Psagot	1981	2,155
Nili	1981	2,148
Barqan	1981	2,119
Bat Ayin	1989	1,814
Kfar Tapuah	1978	1,673
Beit Horon	1977	1,434
Kfar Etzion	1967	1,390
Nofim	1987	1,315
Shavei Shomron	1977	1,112
Rosh Tzurim	1969	1,056
Kiryat Netafim	1983	999
Matityahu	1981	969
Migdal Oz	1977	592

3.1.2 FORMAL STUDY AREA

To reduce processing times and model complexity, the West Bank was subdivided into smaller study areas, focused on the initial set of ten settlements. These areas were initially generated from settlement borders created by PeaceNow.org, the largest and longest-standing Israeli organisation advocating for peace through public channels (Peace Now, 2024; *Peace Now Who We Are*, n.d.). A buffer of 4 km from the settlement polygons was determined to be appropriate to adequately capture geographic diversity while reducing the overall area of modelling. The 4 km buffer was then converted to a rectangular feature envelope for ease of raster analysis. More settlements within the feature envelope were then selected to be studied (Table 1) (Figure 3-1).

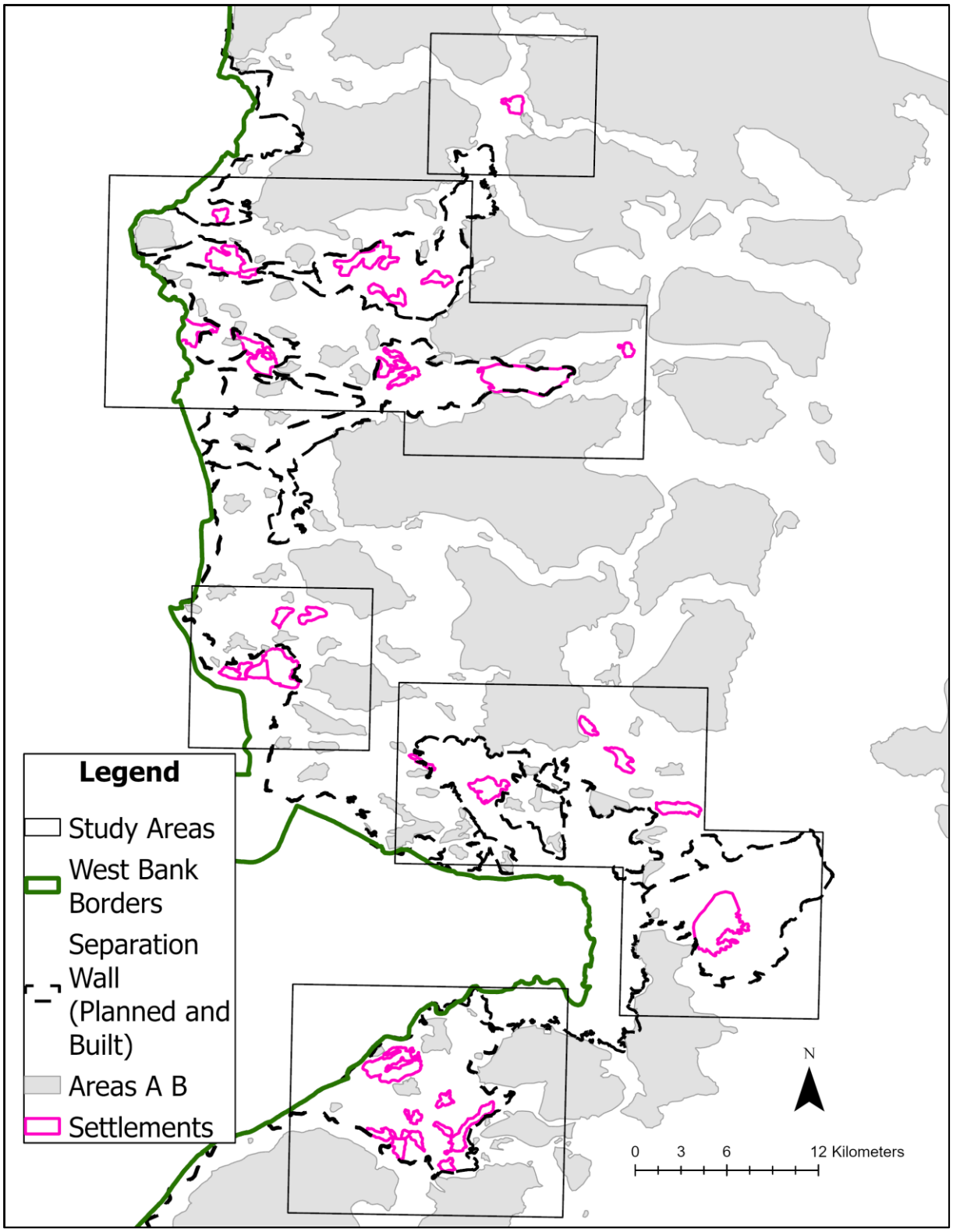

Figure 3-1. Assessed Settlements, with Separation Wall (dotted black), Areas A/B (grey), and West Bank Borders (green). Settlements in pink are those assessed in the study.

3.1.3 TEMPORAL SPAN

To assess the spatial development of built-up area in Israeli settlements, the dates of 1994, 2014, and 2024 were selected. The two modern dates of 2024 and 2014 were chosen to reflect current conditions and as intermediary step, respectively. 1994 is a prominent date due to its proximity to the major policy decisions of the Oslo Accords, which were formed in 1993 and finalized in 1995 (Helal & Zawawi, 2024; Muhsen, 2017). The Oslo Accords had major ramifications for the legality of Israeli expansion into Palestinian territory, influencing settlement growth from then on (Muhsen, 2017). Hence, 1994 was found to be an excellent starting position due to this policy.

3.1.4 ANCILLARY DATASETS

Several vector datasets were employed for ease of analysis and masking of imagery (Table 2). Settlements and outposts were used to create the initial area of interest through a buffer and feature envelope process (section 3.1.2). The West Bank borders were used to mask out non-contested Israeli land (land west of the Green Line) that were not of interest to the final model. Areas A, B and the settlement wall were used as constraint layers for preventing future settlement growth. Major roads were masked from the dataset as they were determined to detrimentally impact final classification and prediction results of built-up land; the model could not adequately separate major roads from built up industrial and residential communities. Finally, a modern satellite basemap was used to assist in validating data to current, on the ground realities.

Table 2. Ancilliary datasets used in the research.

Name	Description	Source
Settlements and Outposts	Polygonized borders of settlements throughout the West Bank. Includes metadata on names in English and Hebrew, settlement type, and time of establishment.	Ofran, H. (2024). Peace_Now_Layers, ArcGIS Online.

West Bank Borders	Polygons of administrative regions belonging to the Palestinian territory and disputed with Israel in the West Bank region.	Esri. (2025). World Administrative Divisions, ArcGIS Living Atlas.
Areas A, B 1995	Polygonized outlines of Areas A, B as established in the Oslo Accords of 1995.	Ofran, H. (2024). Peace_Now_Layers, ArcGIS Online.
Separation Wall	Built and planned elements of the separation wall in the West Bank.	Ofran, H. (2024). Peace_Now_Layers, ArcGIS Online.
Major Roads	Primary roads, filtered to the West Bank region, that were visually large enough to appear in 30m satellite resolution.	OpenStreetMap contributors. (2014). Israel and Palestine, Geofabrik.de.
'World Imagery' Basemap	One meter or better very high-resolution imagery worldwide.	Esri, Vantor, Earthstar Geographics, & GIS User Community. (n.d.). World_Imagery [Dataset].

3.2 SATELLITE DATA

Satellite data for the years 1994, 2014, and 2024 were captured using Google Earth Engine (GEE) and processed with GEE and R. Satellite data was captured from Landsat-5 for 1994, and Landsat 8-9 for 2014 and 2024 at 30-meter resolution. Satellite data was gathered exclusively from Landsat level 2, collection 2, tier 1

collections as these datasets ensure comparability across the timespan of the study (Gupta, 2025; Sonet et al., 2025). The use of these imagery products ensures harmonization across the timespan of the project, with added bonuses of atmospheric and other data corrections (Rahimi & Jung, 2024, p. 8).

For each year, image composites were created using imagery from January 1st to December 31st. Images were corrected using the 'QA' band, and pixels with cloud dilation, clouds, and/or cloud shadows were removed from the image composite. This ensured that only clear-sky pixels were used for analysis in the final product (Fontana et al., 2023; Pimple et al., 2017) The median value of each pixel from the image collection was then collected for each spectral band (section 3.2.1); this technique helps remove the effect of outliers and improves the overall quality of the image (Badshah et al., 2024; Fontana et al., 2023; Yang & Zhao, 2022). Separately, image composites were also used to calculate variability, as described in section 3.2.2. Finally, the resulting image was clipped to the formal study areas (section 3.1.2). All data used in this study was projected to WGS 1984 UTM Zone 36N CSRS: 32636.

3.2.1 Bands and Band Indices

The primary bands selected for this study were red, green, blue, short-wavelength infrared (SWIR) 1, SWIR2, and near infrared (NIR). Red, green, and blue bands are foundational and used to calculate important spectral indices, whilst SWIR and NIR are useful in discriminating urban and vegetated land, respectively. Other urban studies have also used this workflow and have found success (Singh et al., 2022; Tariq et al., 2022; A. Zhang et al., 2025).

Spectral band indices were calculated using the R 'terra' package. Spectral indices can be important to RF classification workflows as they offer normalized insights that aid model performance. Many different indices were selected to aid RF model processing, based on a review of the literature. These were NDVI (Sonet et al., 2025), MNDBI (Sonet et al., 2025), MNDWI (A. Zhang et al., 2025), dry bare-soil (DBSI) (Rasul et al., 2018), enhanced vegetation (EVI) (Mehra & Swain, 2023), normalized burn ratio (NBR) (Rasul et al., 2018), soil-adjusted vegetation (SAVI) (A. Zhang et al., 2025), and normalized-difference moisture (NDMI) indices (Rasul et al., 2018).

3.2.2 Temporal Indices

Time-variable bands were also calculated using GEE. These bands are calculated from the variability and standard deviation of various images taken throughout each year of study to assist in differentiating agricultural land and natural vegetation. Htitiou, A., Boudhar, A., Chehbouni, A., & Benabdelouahab, T. (2021) mention the use of phenological cycles and variability of indices dependent on the growing season of crops to better differentiate between agricultural land and other land uses. Ergen, M. (2025) mentions that multitemporal satellite images can help illustrate seasonal variations in land use classes. In this study, the intra-annual standard deviation of the following indices was used in the RF classification: NDVI, EVI, NBR, SAVI, and NDMI. For NDVI specifically, the NDVI CV (coefficient of variation), amplitude, and variation in monthly peaks were also calculated.

3.2.3 Texture Indices

Image texture indices were also calculated using R to aid in discriminating between land use classes. Tariq et al., (2022) found that identifying a textural difference between bare and built lands helped their classification. Ruiz Hernandez, I. E., & Shi, W. (2018) find that texture metrics helped immensely with the classification of urban land use. In this research, the texture indices of contrast, variance, and entropy were calculated from the GLCM (gray level co-occurrence matrix) for the NDVI and SWIR1 bands to aid in differentiating agricultural and built lands.

An initial run of the RF models was used to determine variable importance, using the ‘permutation’ tool in the ‘ranger’ R package. After this run, three variables were removed from the classification and the RF algorithm was rerun for each year: ‘built_SWIR_entropy’, ‘built_SWIR_dissimilarity’, and ‘veg_NDVImean_homogeneity.’ A comprehensive list of the spectral, temporal, and texture indices used in the dataset can be found in the Appendix B.

3.3 Data Engineering

Several classification rules were applied to the dataset and implemented to aid in the final LULC maps accuracy and interpretability. These rules are described in this section.

3.3.1 LAND USE – LAND COVER (LULC) STRATIFICATION

The dataset was stratified into five different LULC classes, farm, bare, vegetation, built, and settlement (Table 3). Water was also selected as a land use category, however after study area masking, no significant water bodies remained in the study area, and it was removed as a category.

Land use was visually assessed with different band and spectral index combinations in ArcGIS Pro. To help in the visual assessment of different land use classes and serve as a ground-truthing, a reference 2016 LULC dataset created by the Palestinian Ministry of Agriculture was used (Ministry of Agriculture, 2016), as well as high-resolution basemap imagery from ArcGIS (Table 2).

'Settlement' areas were defined as built land that fell within a settlement polygon, as defined by the 'Settlements and Outposts' layer (Table 2). Further, contiguous areas of 'built' pixels that were connected to settlement pixels but did not intersect Area A/B were also included; pixels within Areas A/B would be Palestinian and not of interest to the thesis. To ensure all built pixels were counted within a settlement, the settlement polygons were manually edited so that they contained all the built land within and connected to the initial polygon, but not to built land in Area A/B.

Polygons of homogenous land classes were created and then randomly sampled with points using the 'spatSample' function from the Terra package. Polygon quantities and the number of point samples produced were manually balanced as much as possible to ensure no land class was severely over/underrepresented in the model (Appendix C).

A seed of '123' was generated before random number generation to ensure reproducibility of results.

Table 3. LULC classes and general descriptions.

Land Classification	Description	Code

Farm	Land used for agricultural purposes. Within the dataset, agricultural land presented primarily in large patchworks of monoculture land, and then more confusing small-holder and informal agricultural practices, such as olive tree plantations.	1
Bare	Land devoid of all vegetation. This was very apparent in the deserted lands in the east of the dataset, and in areas cleared for construction.	2
Vegetation	Land with some vegetation, determined to be not agricultural. Vegetated land includes forest and shrubland, which were very common across the dataset.	3
Built	Land with human-made structures, such as houses, concrete, patchworks of roads, and buildings. Urban land had to be a significant patchwork to be recognised in the model, so this excluded disconnected buildings and large roads without buildings.	4
Settlement	Built land within and connected to settlement polygons, as defined by the 'Settlements and Outposts' shapefile.	5

3.3.2 MAJORITY AND TEMPORAL FILTERING

After land use classification, a 5x5 majority filter was applied. Majority filters help reduce 'salt-and-pepper' effects and can help increase the homogeneity of the classified image. Ergen, M. (2025) uses a majority filter to further improve the accuracy of their classification. Duan, X et al., (2025) use a 4x4 and 8x8 majority filter to eliminate isolated pixels and increase their model accuracy. Different majority filter sizes were experimented within the model, but the 5x5 filter was found to reduce the amount of 'salt-and-pepper' and increase the spatial homogeneity without reducing final model accuracy metrics.

To increase temporal consistency across the dataset, several transition rules were employed. Temporal filtering of results for consistency and accuracy is useful in ensuring LULC classification consistency across long timespans (Gómez et al., 2019; Qian et al., 2020). The first ruleset applied to land classified as 'Settlement'. Four rules were implemented, based on the key assumption that no major demolitions occurred within the settlements of interest during the study period. This assumption is supported by the literature, as most demolitions occur within unauthorized outposts and growth – and these demolition orders are mostly ignored anyways (Ofran & Shem-Tov, 2017). The next rule applies to farm and vegetation land that flickered in

2014, as compared to a baseline in 1994 and 2024. This rule was implemented due to the spectrally mixed nature of these land classes. Metrics illustrating the exact magnitude of change and specific rules can be found below (Table 4).

Table 4. Temporal Filtering Rules. $\boldsymbol{P_X}$ refers to a pixel from a year of interest.

#	Rule	Assumption	% of pixels re-classified of land class	% of pixels reclassified of total
1a	$if\ \ P_{1994} = settlement\ \&$ $P_{2014} = settlement\ \&$ $P_{2024} = non-settlement\ THEN$ $P_{2024} = settlement$	Assume settlement was not demolished after 2014.	2.02	0.07
1b	$if\ \ P_{1994} = settlement\ \&$ $P_{2014} = non-settlement\ \&$ $P_{2024} = non-settlement\ THEN$ $P_{1994} = non-settlement$	Assume settlement was not demolished after 1994.	9.92	0.14
1c	$if\ \ P_{1994} = settlement\ \&$ $P_{2014} = non-settlement\ \&$ $P_{2024} = settlement\ THEN$ $P_{2014} = settlement$	Assume pixel did not transition in 2014 and revert in 2024.	3.74	0.10
1d	$if\ \ P_{1994} = non-settlement\ \&$ $P_{2014} = settlement\ \&$ $P_{2024} = non-settlement\ THEN$ $P_{2014} = non-settlement$		6.69	0.18
2a	$if\ \ P_{1994} = vegetation\ \&$ $P_{2014} = farm\ \&$ $P_{2024} = vegetation\ THEN$ $P_{2014} = vegetation$		6.93	1.39
2b	$if\ \ P_{1994} = farm\ \&$ $P_{2014} = vegetation\ \&$ $P_{2024} = farm\ THEN$ $P_{2014} = farm$		13.27	6.42

3.4 RANDOM FOREST (RF)

The RF algorithm is a ensemble supervised classifier that utilizes Classification and Regression Trees (CARTs) to produce predictions (Breiman et al., 2017). It has become increasingly popular in remote sensing, and especially within urban growth

prediction modelling due to its high performance and stability in classification tasks (Badshah et al., 2024). A meta-analysis of almost 350 peer-reviewed remote sensing papers found that random forest was the most commonly used algorithm for interpretation of satellite imagery in the past decade (Badshah et al., 2024).

In this research, Random Forest was implemented using R and the 'ranger' package. 'ranger' offers advantages due to its fast speed and efficient memory usage compared to other RF packages (Demir & Sahin, 2023).

To select the optimal hyperparameters for the RF model, it was decided that a grid search with k-10 cross validation would supply the least biased results. Three hyperparameters were tested for using a grid search: *mtry, sample fraction*, and the *minimum node size*, which were noted to have the most impact on random forest model performance (Probst et al., 2019). *Mtry* determines the number of candidate variables assessed by the model at each split (Probst et al., 2019). *Minimum node size* is also noted to be influential on model performance, most especially processing times, where larger values can increase model speeds without increasing errors (Probst et al., 2019). The *sample fraction* should also be tuned, smaller values lead to less correlated trees (Lovelace et al., 2019). *Ntree* is another hyperparameter often influential and tested for, however it was not tested for in this paper as *Ntree* does not impact results to the same degree as *Mtry*, and classification results stabilise at higher values (>500) without risk of overfitting (Belgiu & Drăguţ, 2016).

3.4.1 Parameters and Accuracy Assessment

For each year of study, training samples were randomly sampled from their polygons with a seed of '123' for reproducibility. Model training and hyperparameter tuning were conducted on the 70% subset, and 30% of the data was used for final accuracy testing after classification and filtering.

Cross validation was performed with k = 10 folds. A grid search was performed using an inner model, using an *Ntree* of 300 to evaluate hyperparameters from the grid search. The optimal hyperparameters were determined to be *mtry* = *5*, *minimum*

node size = 1, and *sample fraction* = 0.8 for all years. A final RF model was then ran using these optimal hyperparameters and *Ntree* of 1000.

Majority and temporal filtering were then applied on the classified raster. After a final evaluation on the initial test data set, a confusion matrix was generated for each year. The confusion matrix produces multiple accuracy metrics, including overall accuracy (OA), User's Accuracy, Producer's Accuracy, and the kappa co-efficient.

3.4.2 LULC Change Dynamics

LULC change was calculated using R. Change between 1994 – 2014, 2014 – 2024, and 1994 – 2024 was analysed. To calculate the amount of change per land class, the area of the total quantity of pixels of each class for the initial year was subtracted from the area of the total quantity of pixels from the latter year. Transitions to each land class was calculated using cross-tabulation matrices. Rate of change was also calculated for each temporal period per each land class to help in understanding land dynamics over time and quantify scenarios.

3.5 Predictive Modelling of Settlement Growth

Predictive modelling of settlement growth was performed using the Land Change Modeller (LCM) module in the Terrset IDRISI LiberaGIS software. The LCM is a powerful module commonly used by the current literature to predict urban growth (Abuelaish, 2018; Abuelaish & Olmedo, 2016; Badshah et al., 2024; Bashyal et al., 2024). The software predicts the state of LULC at a time T3, based on historical change from time T1 and T2. It accomplishes this using an empirically driven stepwise process with three primary steps: change analysis, transition potentials calculated from submodels, and change prediction using CA-Markov and change allocation algorithms (Girma et al., 2022). The 'Change Analysis' section simply calculates area and locations of transitions between each land class present in the historical images.

In the subsequent step, transition potentials of interest are modelled using explanatory variables, referenced here as 'drivers', and submodels. Submodels are constructed through machine learning algorithms: of which there are six available in the LCM infrastructure: Multi-layer Perceptron (ANN), DecisionForest (DF), Logistic

Regression, Weighted Normalized Likelihood (WNL), SVM, and SimWeight. Typically, most papers reporting on using LCM use the MLP module, however the DecisionForest model was determined to give the best predictive results for this research. Results comparing DecisionForest and other model performance can be found in Appendix D.

3.5.1 DRIVERS OF TRANSITION

The prediction of transitions of land use classes to settlement land requires an understanding of 'drivers' of change, or independent variables that may influence how land will change over time. In this study, ultimately nine driver variables were selected for the model (Figure 3-2). Data sources for each driver are also listed in Appendix E. All distance variables use Euclidean calculations to define how close and far away drivers were to each other.

Distance to barriers is the distances to Areas A and B, within Area C. These areas can significantly affect urban growth, as settlers are legally obligated not to build within Areas A and B (Sbaih & Thawaba, 2025). Urban development must then only occur within the confines of Area C (Sbaih & Thawaba, 2025). The barriers also include the separation wall, which is another significant constraint to settlement growth (Nassar et al., 2019). Distance to cities and towns can impact growth as they serve as proximity to urban centres. Settlements may be incentivized to grow closer to urban centres due to ease of ability of purchases and access to services that would not be available within the settlement (Abuelaish, 2018). Railways can be significant sources for urban growth to occur, as they allow ease of access throughout the region (Kasraian et al., 2019). Elevation can significantly aid in predicting urban growth as land use planners may wish to build on flat land with gentle slopes (Chouhan & Shekhawat, 2025). The same reasoning can then be said of the Slope driver. For settlements, planners may have also prioritized high elevations for surveillance and control purposes (Ghodieh, 2020).

Roads may be the most significant driver for predicting urban growth. Much population is built along roads, and they also serve as a planning element, where future growth will occur on roads without any current built area (Abuelaish, 2018). Further, the data for the roads was slightly modified, where extraneous roads, such

as footpaths, trails, and tracks, were deleted to aid predictive power. Finally, waterways can also serve as powerful predictors of urban growth, especially in desert areas like the West Bank where water can be scarce (Muhsen, 2017). Further, settlements are built as ways of controlling Palestinian territory, and increasing control of water sources can influence the direction and magnitude of Israeli settlement growth (Muhsen, 2017).

Other drivers were considered but ultimately excluded from the model as they did not meaningfully increase the accuracy and skill of the model and ultimately hurt final model validation metrics. This included population density, which was constructed roughly using 1994 population statistics and classified settlement lands from the Random Forest process. Evidence Likelihood is another popular driver that expresses the probability of finding change between settlement land and all other land classes in a pixel (Mustak et al., 2022). Some studies source it as a very powerful, or their most powerful, driver, however this success was not replicated within this study (Bashyal et al., 2024).

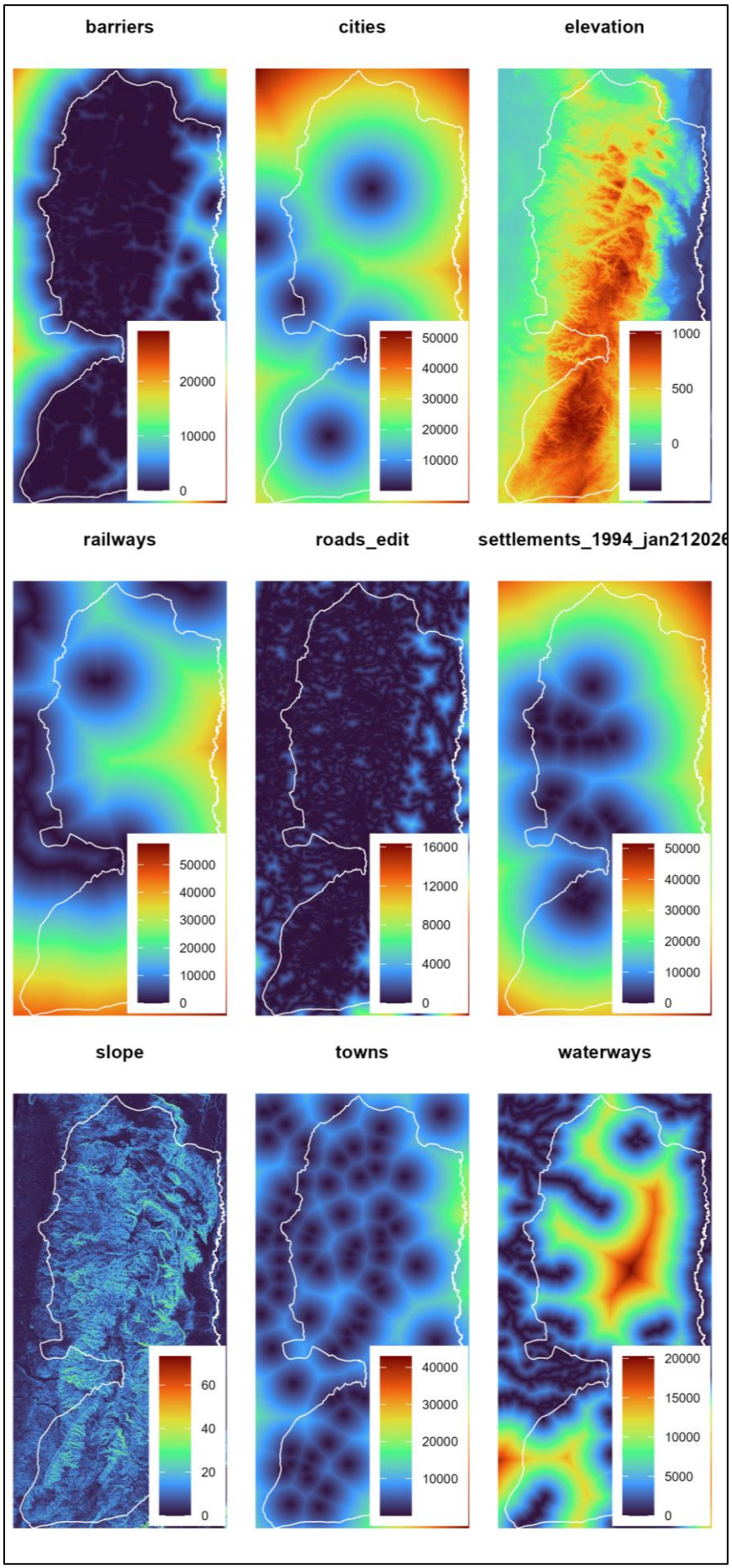
barriers
20000
10000
0
cities
50000
40000
30000
20000
10000
elevation
1000
500
0
railways
50000
40000
30000
20000
10000
0
roads_edit
16000
12000
8000
4000
0
settlements_1994_jan212026
50000
40000
30000
20000
10000
0
slope
60
40
20
0
towns
40000
30000
20000
10000
waterways
20000
15000
10000
5000
0

Figure 3-2. Driver variables used in the study. Distances are in meters. The white line represents the political borders of the West Bank. From top left to bottom right; distance to barriers, distance to cities, elevation, distance to railways, distance to roads, distance to 1994 settlement areas, slope (%), distance to towns, and distance to waterways.

3.5.2 MODEL SPECIFICATION

As stated in the earlier section, there are multiple models available within the LCM infrastructure that allow for the submodelling of transitions. In this study, it was found that the DecisionForest algorithm was adept at producing good Out-of-Bag (OOB) accuracy and skill and had the best performance when validated with 2024 actual LULC data (Appendix D).

Three land transitions were modelled using DecisionForest: farm to settlement, vegetation to settlement, and bare to settlement. The Decision Forest model has three parameters that can be modified by the user. The first is the sample size, which was maintained at their default values. Secondly is the number of variables considered at a split of a tree. The default value for this was 2, however its maximum value can be set to equal the number of drivers in the dataset. Ultimately, the value of '4' gave the best results consistently. Similarly, the number of trees was also selected to be 500, with a default value of 100. 500 was found to be the best medium between the model processing time and accuracy.

The LCM provides values that aid in the assessment of model performance. These are the OOB model accuracy and skill. OOB accuracy simply refers to the accuracy calculated with validation data held back (50% of the data in TerrSet) (Eastman, 2024). Skill is the measured accuracy of the model minus the accuracy expected by change (Eastman et al., 2024). Values closer to 1 indicate the model is performing 'skillfully', while closer to 0 indicate the model is behaving randomly (Sisay et al., 2023). There is also an iterative process where the model keeps one driver variable constant while modifying the weights of the other drivers. If the accuracy and/or skill of the model is significantly impacted by keeping a driver constant, it would imply the driver impacts the model greater than other drivers.

3.5.3 CALCULATING SETTLEMENT GROWTH

To quantify the annual amount of change that occurred within a settlement, the extent of the settlement was manually defined using visual assessment. All pixels classified as 'settlement' within the individual settlement polygon were then counted for 1994, 2014, and 2024, producing a growth rate for each individual settlement. The formula used to calculate the annual growth rate is the Compound Annual Growth rate (CAGR) equation, given below (Ergen, 2025):

$$CAGR = \left(\frac{A_{t\,1}}{A_{t0}}\right)^{\frac{1}{n}} - 1 \qquad (Eq\ 1)$$

Where $CAGR$ is the compound annual growth rate, A is the area of the settlement, $t1$ is the final time of evaluation (2024), $t0$ is the initial year of evaluation (1994), and n is the number of years between the initial and final times of evaluation.

3.5.4 SCENARIOS

To assess how settlement growth may respond under different Israeli policy regimes, three settlement-expansion scenarios were implemented using the Change Analysis module of the LCM: Business-as-Usual (BAU), Low-growth/High-constraint, and High-growth/Low-constraint. CAGRs for settlement expansion over the period 1994–2024 were first calculated, and their statistical distribution summarized using the minimum, 25th percentile, median, 75th percentile, and maximum values. The 25th and 75th percentile values were used to parameterize the low-growth and high-growth scenarios, respectively. Each percentile value was normalized by the median CAGR to derive a scalar (Eq. 2), which was applied to the Markovian settlement transition probabilities by multiplying it to all transitions into the settlement class. The sum of the row of the transition matrix must equal 1, so the difference was added/subtracted from the persistence class in the matrix.

Using statistical quartiles to define low- and high-growth scenarios grounds the model in empirically observed variability rather than arbitrary numbers. Under the BAU scenario, a constraint was applied to expansion within Areas A and B and within a 30-m buffer surrounding the settlement wall. In the low-growth scenario, these

spatial constraints were expanded by an additional 500 m, further limiting areas available for expansion. In contrast, the high-growth scenario removed all spatial constraints, representing a policy environment with minimal regulatory restrictions.

$$S = \begin{cases} \frac{Q_{25}}{g} \; Low - growth\; scenario \\ 1 \;\; Business - As - Usual \\ \frac{Q_{75}}{g} \; High - growth\; scenario \end{cases} \qquad (Eq\ 2)$$

Where S is our scalar, g is the median value of the CAGR, Q_{25} is the bottom 25% quartile CAGR, and Q_{75} is the top 75% quartile. Values below the median will be lower than 1, and apply a decreasing effect on the transition matrix, while values above the median will be greater than 1, and apply an increasing effect.

3.5.5 Directionality and Intensity of Change

The direction and intensity of urban growth is also quantified, which aids in understanding of where settlements are growing most strongly. Other studies quantify the directionality of urban growth using azimuths (Rimal et al., 2020), and kernel density estimation (KDE) to estimate intensity of urban growth (Souza et al., 2025). To establish the relative intensity of urban growth in settlements, ArcGIS Pro was used on actual 1994, 2024, and predicted BAU 2054 settlement images. 1994 – 2024, and 2024 – 2054 settlement extents were compared by computing the absolute difference between either image. These change rasters were then converted to vector points. Then, the kernel density tool was run using these points with a search radius of 1000 meters.

Directionality of change was calculated in R. The center point was determined to be the geographic center of the 1994, 2024, and 2054 settlement extent rasters. Then, the study area was subdivided in 24 sectors, each representing 15-degree portions around the center point. KDE values were aggregated within each 15-degree portion to estimate the relative intensity of urban growth of each direction around the center-point. We illustrate this with a rose diagram, where longer ‘petals’ indicate greater KDE values within that direction.

3.5.6 VALIDATION OF MODEL OUTPUT

In the 'Change Planning' tab of the LCM, multiple parameters can be adjusted to create the model prediction and validation of the model output. The model was ran using the submodels produced in the previous transition modelling steps, with a prediction date set to 2024. The outputs of this model are a 'hard' transition and 'soft' transition. The hard transition map is based on the output of a competitive land allocation model, which defines a commitment to the best guess of which land will actually transition where (Eastman et al., 2024). On the contrary, the soft prediction map outputs areas with high and low probabilities to change, like a map of vulnerabilities for the modelled transitions (Eastman et al., 2024).

To understand how well the predictive model performs on real data, validation of the predicted data was performed using real data. Here, the predicted 2024 map was validated with the actual 2024 map. There are several important validation metrics that are commonly used in other urban prediction papers, described in the below sections.

3.5.6.1 ACCURACY OVER SETTLEMENT SPACE

Many papers in the urban prediction field report overall predictive accuracy – which compares the quantity of correctly predicted pixels in the predicted image versus the actual image. This metric and the Kappa coefficient are very commonly implemented in many urban and land prediction papers due to its typical high reported values (Duan et al., 2025; Singh et al., 2022; A. Zhang et al., 2025). However, it is important to note that most of this value comes from the persistence of pixels from the two time periods and should be interpreted with care.

In this research, the accuracy over the settlement space is reported. The calculation of the settlement space is simply the union of the actual and predicted settlement pixels. The accuracy over the settlement space is then the quantity of predicted pixels divided by the size of the settlement space (equation 3). This metric helps give a more accurate comparison of the accuracy of the model.

$$Accuracy_{Settlement\ Space} = \frac{Number\ of\ predicted\ settlement\ pixels}{Actual\ settlement\ pixels \cup Predicted\ settlement\ pixels} \qquad (Eq\ 3)$$

3.5.6.2 METRICS OF DISAGREEMENT

Quantity disagreement and allocation disagreement are two metrics that quantify the disagreement space of the predictive model, and in recent times are more preferred than traditional accuracy and uninterpretable kappa metrics (Pontius Jr & Millones, 2011). Quantity disagreement is a measurement of the error that results from the less-than-perfect match in the overall proportion of predicted versus actual change in any category (Pontius Jr & Millones, 2011). This is simply the difference in size of the predicted category to the actual category. Allocation difference is defined as the less-than-perfect spatial allocation of a category, given the proportions of the categories in the predicted and actual maps (Pontius Jr & Millones, 2011). These two metrics form the entire disagreement space of the model. The equations for quantity and allocation disagreement are given below, adapted from Pontius Jr & Millones (2011).

$$q_g = \left|\left(\sum_{i=1}^{J} P_{ig}\right)\right| - \left|\left(\sum_{j=1}^{J} P_{gj}\right)\right| \qquad (Eq\ 4)$$

$$\alpha_g = 2\min\left[\left(\sum_{i=1}^{J} P_{ig}\right) - P_{gg}, \left(\sum_{j=1}^{J} P_{gj}\right) - P_{gg}\right] \qquad (Eq\ 5)$$

Where q_g is the quantity disagreement for any given random category *ig* or *ji* in the reference or comparison maps, and α_g is the allocation disagreement for any random category *ig* or *gj.* More information on these formulae can be found in Pontius Jr & Millones, (2011).

3.5.6.3 FIGURE OF MERIT (FOM)

The Figure of Merit (FoM) is the final metric reported within this project. The FoM is a simple measure that quantifies that percentage of correct predictions that occurred within the predicted map. It is defined below (equation 6), where the numerator is the intersection of predicted and observed change, and the denominator is the union of the prediction and observed change (Varga et al., 2019):

$$Figure\ of\ Merit\ (FoM) = \frac{Hits\ (100\%)}{Misses + Hits + False\ Alarms} \qquad (Eq\ 6)$$

Misses are areas that transitioned that were not captured in the prediction, hits are areas of correctly predicted change, and false alarms are areas that were predicted to change but did not. Because we are only predicting areas that transitioned to a singlular class ‘settlements’, we omit the variable ‘wrong hits’ from the denominator, which define areas correctly predicted to change but classified as the wrong land use.

FoM is not as regularly reported in urban prediction papers, and its values may vary wildly between research contexts due to the amount, area, and complexity of land classes predicted.

The final methodological flowchart is shown in Figure 3-3.

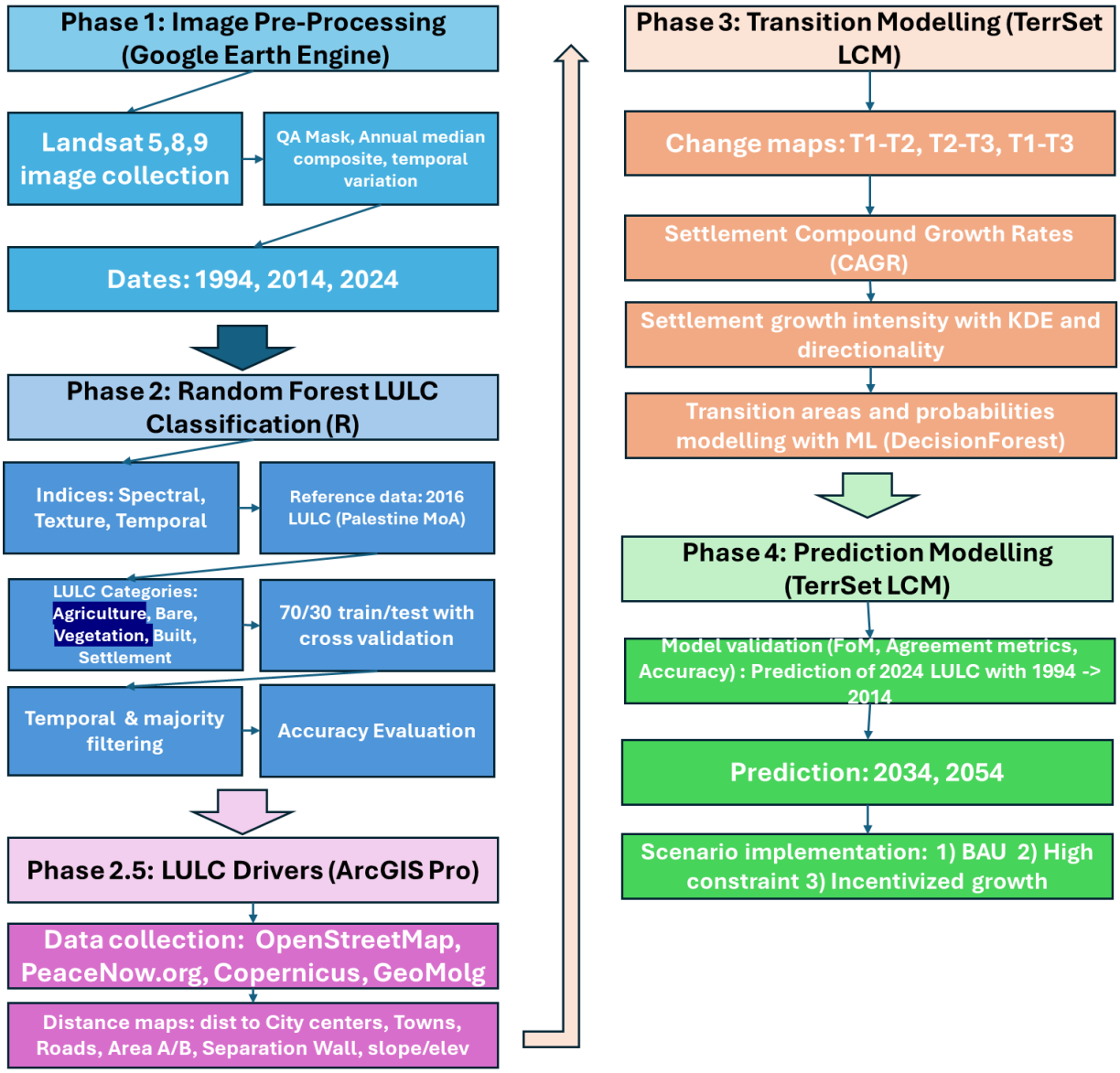

Figure 3-3. Methodological flowchart.

4 RESULTS

4.1 Random Forest Classification Accuracy

Confusion matrices were constructed for the classified random forest maps for 1994, 2014, and 2024 after majority and temporal filtering. From these confusion matrices, the producer accuracy, user accuracy, kappa coefficients, and overall accuracy for each year were calculated (Table 5). The settlement class was not included in the confusion matrices, as it was manually classified after random forest, and hence would be inflating accuracy values. Here, they are included within the 'Built' land use case.

Overall classification accuracy for the study area was 90.3% for 1994, 90.7% for 2014, and 88.3% for 2024. The classifier generally classified built and bare lands well, at accuracies over 90%. However, it struggled to classify the land classes of agriculture and vegetation, reporting lower values of 75 – 80%. This is most likely due to the mixed nature of these pixels, and also due to the large quantity of small-holder, informal farming common in the West Bank (Ghodieh, 2020). Mixed areas, such as vineyards, were difficult to differentiate between. Further, olive farms are another common agricultural practice, and these have very similar spectral identities to forested and vegetated land.

Table 5. Random Forest Accuracy Evaluation for 1994, 2014, and 2024

		Years		
	Variables	**1994**	**2014**	**2024**
Producer Accuracy	*Agriculture*	94.21	94.83	90.52
	Bare	94.44	98.40	95.61
	Vegetation	82.08	73.28	77.12
	Built	89.74	95.31	90.08
User Accuracy	*Agriculture*	80.85	85.94	81.40
	Bare	91.07	92.48	90.08
	Vegetation	95.60	93.41	92.86
	Built	97.22	91.73	90.08
Kappa Coefficient		0.87	0.88	0.84
Overall Accuracy		90.3	90.7	88.3

4.2 LULC CHANGE

The change of agricultural, bare, vegetation, built, and settlement land from 1994, 2014, and 2024 were analysed in this research (Figure 4-1) (Figure 4-2) (Figure 4-3). In all years, farmland consistently remains the highest land use within the study area at 68,852 hectares, representing 64% of all land. However, this proportion decreases to 53% (57,269 ha) in 2014, showing a relative decrease of -16.8% or -11,583 ha, and then to less than half of the dataset at 46% (49,456 ha) in 2024, or a loss of -7,673 ha. Bare land, which narrowly constitutes the second most represented land use in 1994 (14,511 ha) and 2014 (17,402 ha), shows an increasing trend in 2014, then decreases in 2024 (16,935 ha).

The three other land classes of vegetation, built, and settlement land all show consistent upwards trends of growth from 1994 – 2014.

Settlement land, although constituting the smallest portion of the study area at 1.3% of the total area, grows extremely rapidly from 1994 (1,405 ha) to 2014 (2,855 ha), representing a 103.23% relative increase. Its growth slows in 2024 (3,636 ha) at 27.36% but is still the highest relative growth out of all land classes evaluated in the study, and its total proportion more than doubles its 1994 amount at 3.4% of the total study area. Built land shows similar growth rates, rising from 8% of the study area in 1994 (8,535 ha) to 12.7% in 2014 (13,599 ha). This also shows a remarkable relative increase of 59.33% in twenty years, illustrating the high urban growth rates that occurred in the region. In 2024, built growth slows at a 22.41% increase (16,646 total ha). Finally, vegetated land slowly increases from 13,886 ha in 1994 to 16,035 in 2014. It also increases sharply in 2024 with a 27% relative increase to 20,376 ha.

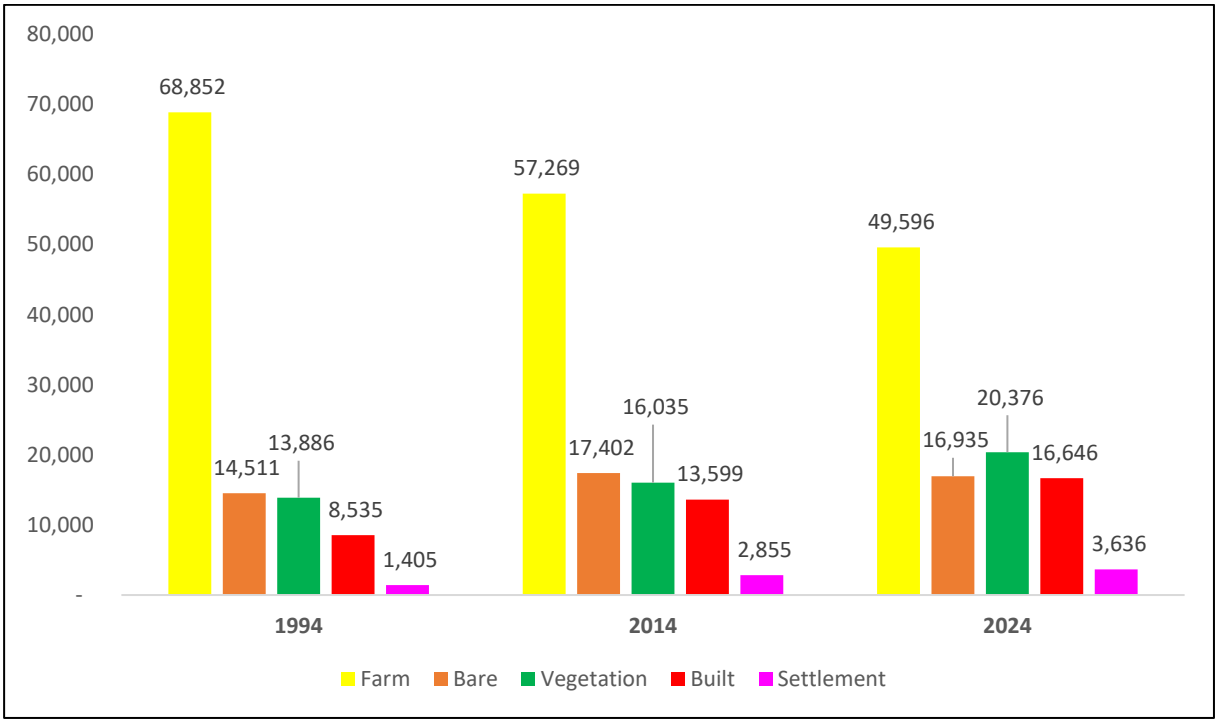

Figure 4-1. Area (ha) of LULC Classes for 1994, 2014, 2024.

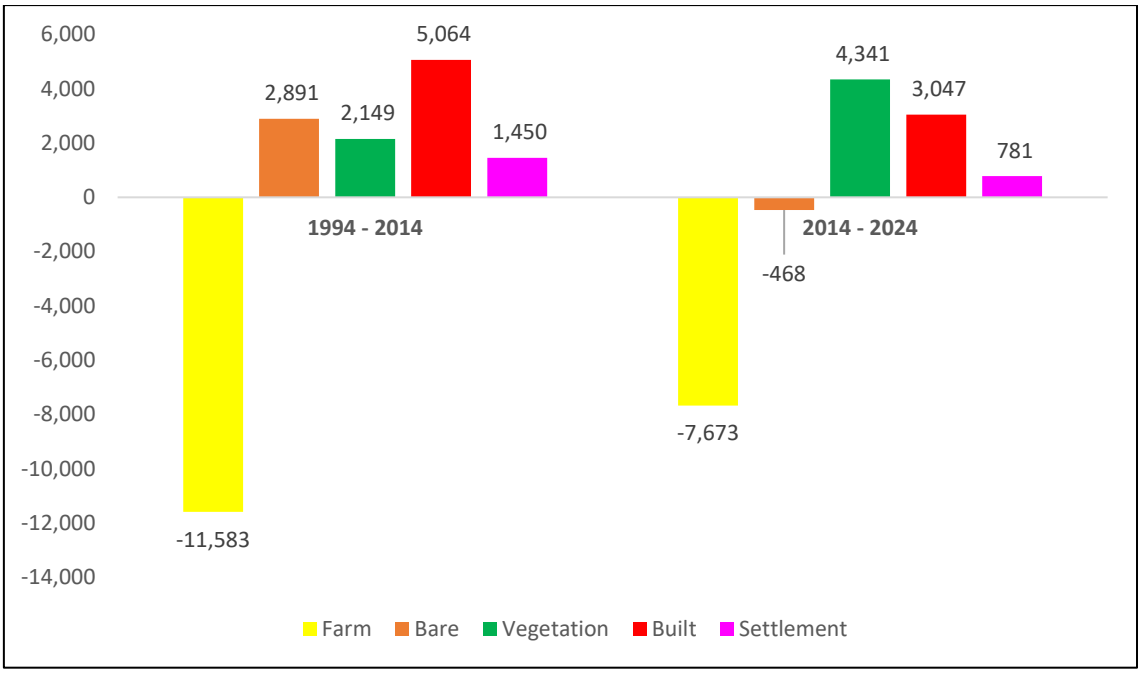

Figure 4-2. Area Change (ha) of LULC classes, 1994 – 2014 and 2014 – 2024.

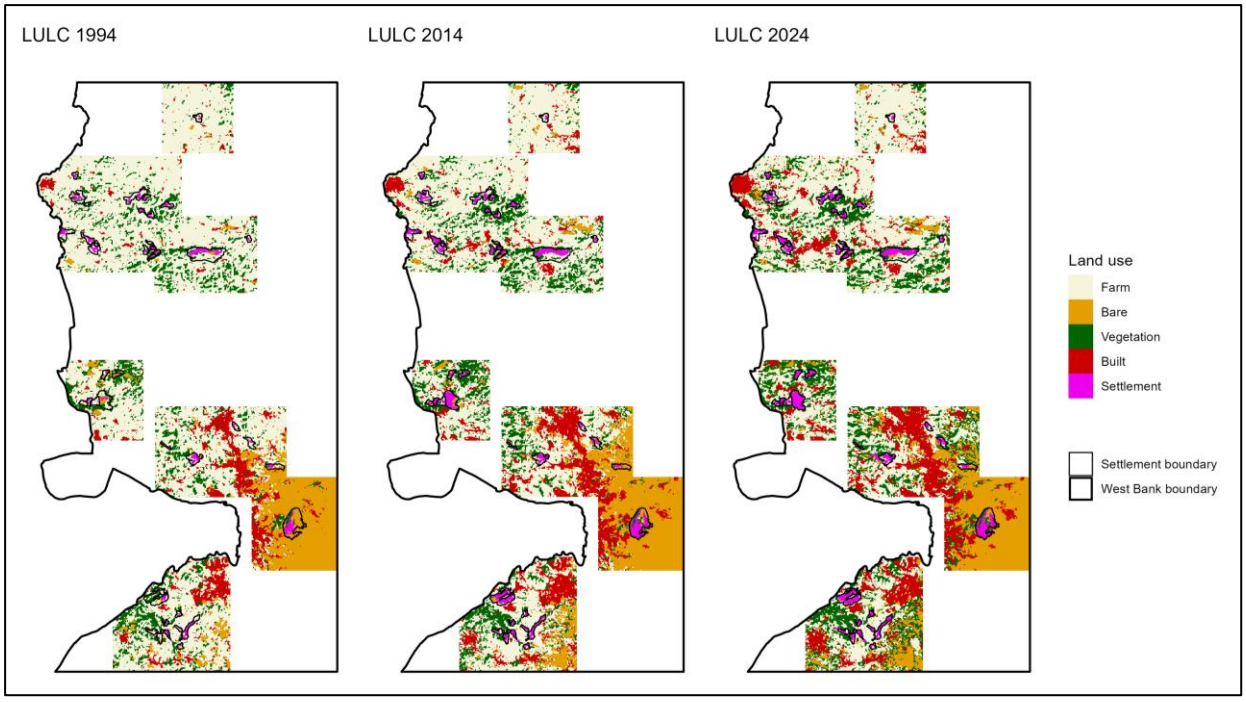

Figure 4-3. LULC classes of the entire study area for 1994 (left), 2014 (middle), and 2024 (right).

4.3 Gains and Losses

Gains and losses of each land cover class were calculated using the terra package in R (Table 6) (Figure 4-4). The largest losses from 1994 – 2014 occur in the Farm

class, with 4,131 ha of land transitioning to bare (3.85% of total land), 5,947 ha to vegetation (5.55%), and 4,836 ha to built (4.51%). It is also the single largest contributor of settlement land growth, with 716 ha transitioning, or 0.67% of total land. The next biggest contributor to settlement growth is bare land, with 479 ha of bare land transitioning, representing 0.41% of the study area. Bare land also contributes significantly to built land at 1,034 ha (0.96% of the total land). This may be representative of construction activity, especially in cleared areas around built-up/settlement pixels. Bare land also shows the highest retention rate between 1994 – 2014 (excluding settlements) at 81.19% of its total area remaining the same, which can be explained the bare, desert lands in the east of the dataset with little development. Vegetation shows no clear trends but does contribute 295 ha (0.28% of the total area) to settlements. A significant amount of vegetation also transitions to farmland at 2,635 ha (2.46%). Vegetated land is also the most variable of the land classes, with only two-thirds (67.09%) of its land being retained in 2014. Built land is the second highest retaining land class, with 81.19% of its 1994 area remaining the same in 2014. It also features transitions to farm, bare, and vegetation, with farm being the highest at 746 ha (0.7% of the total land area).

From 2014 – 2024, there are smaller overall transitions due to the shorter timespan. Farmland contributes the most to settlement growth with 323 ha (0.3% of the total area), then bare land at 292 ha (0.27%), and finally vegetation at 167 ha (0.16%). Settlements increase from 2.66% (2,855 ha) to 3.39% (3,636 ha) of the total study area. Vegetation remains the most variable land class, retaining 77% of its total area, followed closely by bare land (78%), and farm (80%). Built land retains a greater proportion of its land at 85.4%.

Table 6. Transition Area Matrix of LULC Transitions, for 1994-2014 and 2014-2024, in hectares

	2014					
1994	**Farm**	**Bare**	**Vegetation**	**Built**	**Settlement**	**Total**
Farm	53,207	4,131	5,947	4,836	716	68,837
Bare	679	11,810	547	1,034	439	14,509
Vegetation	2,635	832	9,311	806	295	13,879
Built	746	629	228	6,923	-	8,527
Settlement	-	-	-	-	1,405	1,405
Total	57,268	17,402	16,034	13,599	2,855	107,157

	2024					
2014	**Farm**	**Bare**	**Vegetation**	**Built**	**Settlement**	**Total**
Farm	45,961	1,962	5,759	3,263	323	57,268
Bare	831	13,615	1,633	1,031	292	17,402
Vegetation	1,728	1,016	12,392	732	167	16,034
Built	1,062	341	588	11,608	0	13,599
Settlement	-	-	-	0	2,854	2,854
Total	49,581	16,934	20,372	16,635	3,636	107,157

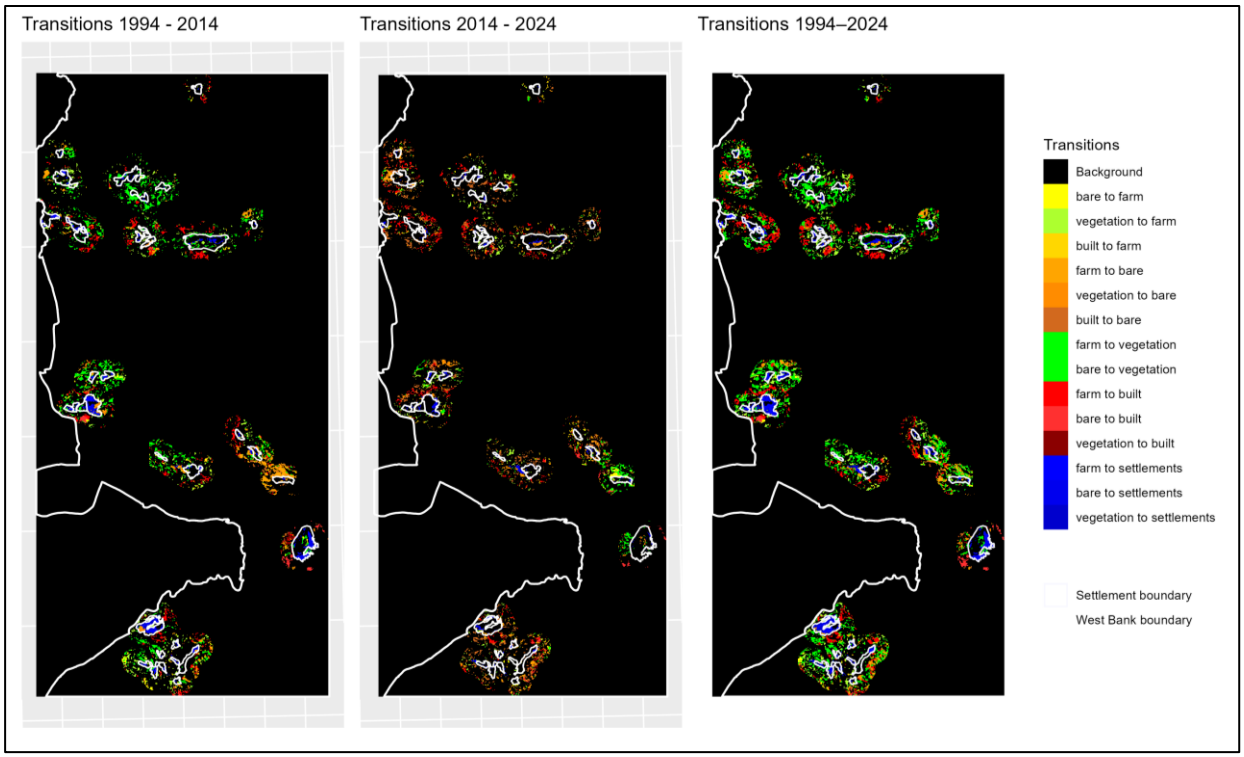

Figure 4-4. Transition areas for 1994 – 2014 (left), 2014 – 2024 (middle), and 1994 – 2024 (right).

4.3.1 SETTLEMENT CHANGE

Individual settlements were analysed for change (Table 7). Overall, there is a clear expansion trend in Israeli settlements from 1994 to 2024 (Figure 4-5). On average, settlements within the study area expanded their area by 49% from 1994 – 2014, and then 34% from 2014 – 2024. The settlement that grew the most in terms of hectares from 1994 to 2024 is Beitar Illit, which increased by 310.99 ha, or a 792% of its original 1994 area. In terms of relative increase, Na'ale grew the most proportionally, from 3.93 ha in 1994 to 68.75 ha in 2024, representing an astonishing 1,651% increase.

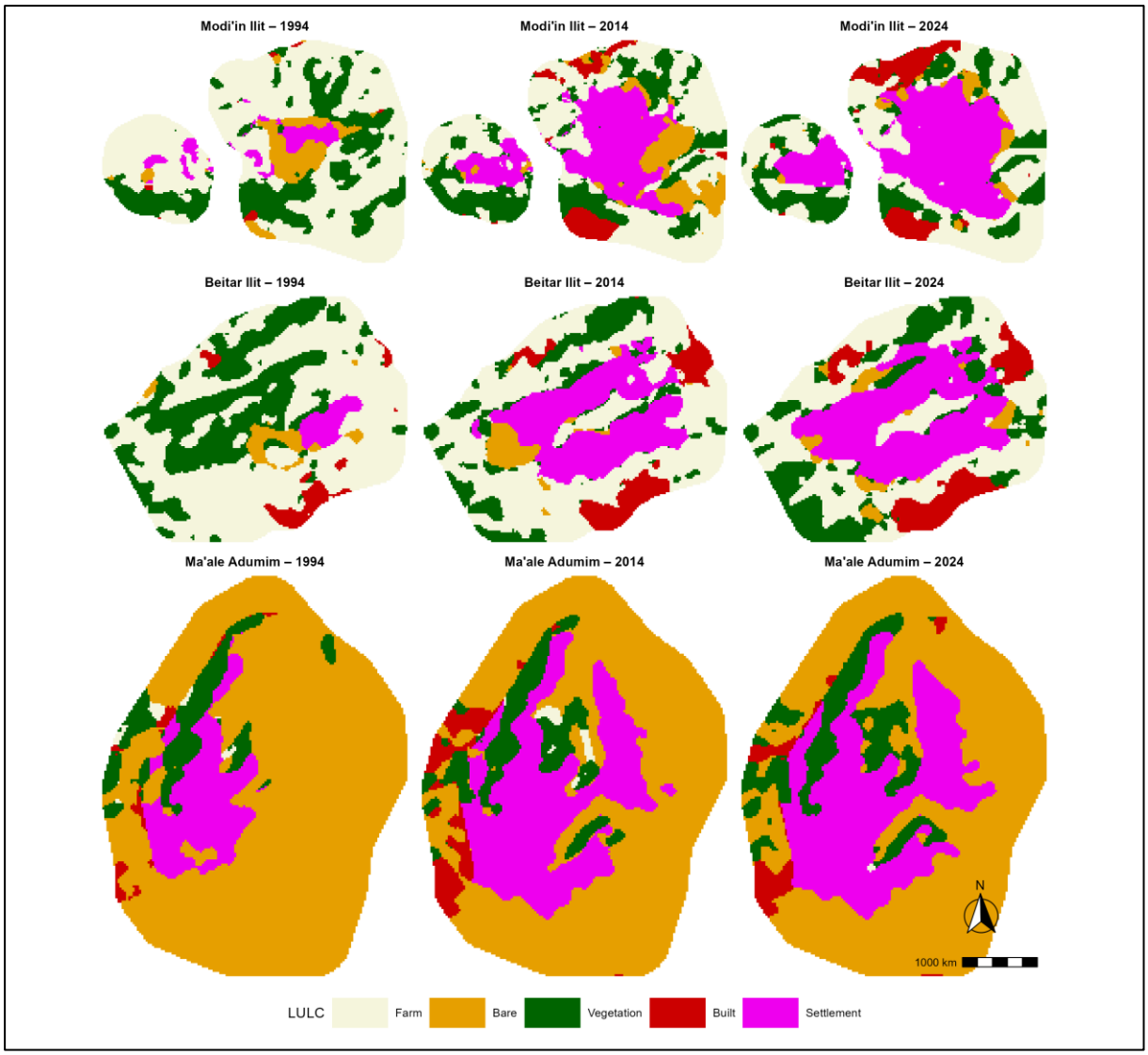

Figure 4-5. Land use – land cover of the major settlements of Modi'in Illit, Beitar Illit, and Ma'ale Adumim, for the years of 1994 (left), 2014 (middle), and 2024 (right).

From these values, the median CAGR was calculated (Figure 4-6). From 1994 – 2014, the average settlement expanded its area by 4.20% annually. From 2014 – 2024, this number slightly lowered to 2.86%. Median annual compound growth rates are similar, at 3.15% from 1994 – 2014, and 2.51% from 2014 – 2024. For the entire time span of 1994 – 2024, the average settlement expanded by 3.74% of its area annually (2.84% for the median settlement). The 25% quartile was 2.27% annual settlement growth, and the 75% quartile was 4.62% annual settlement growth.

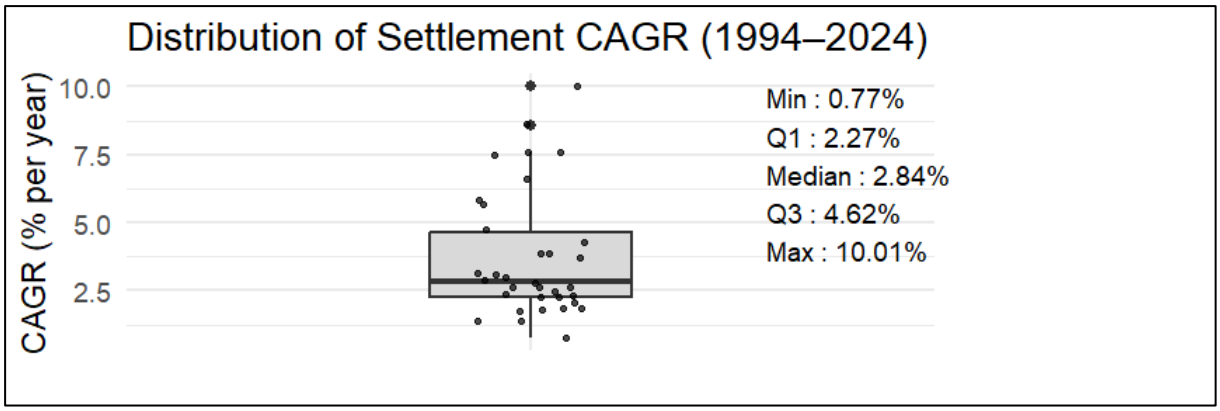

Figure 4-6. Boxplot of CAGR of Settlements from 1994-2024.Black dots are the CAGR for individual settlements in the study area.

Table 7. Settlements and their areas (hectares) and % increases, 1994 - 2014 and 2014 - 2024

Settlement	1994	2014	2024	% increase 1994 - 2014	% increase 2014 - 2024
Alfei Menashe	62.23	96.23	107.09	35%	11%
Alon Shvut	40.18	72.51	86.96	45%	20%
Ariel	194.88	282.00	329.70	31%	17%
Barqan	90.80	127.39	168.23	29%	32%
Bat Ayin	4.34	28.07	51.62	85%	84%
Beit Horon	19.05	35.67	39.84	47%	12%
Beitar Illit	39.26	289.60	350.25	86%	21%
Efrata	95.31	126.22	143.76	24%	14%
El'azar	8.69	34.08	34.83	75%	2%
Elkana	63.65	86.20	124.55	26%	44%
Geva Binyamin (aka Adam)	35.42	42.94	61.06	18%	42%
Giva'at Ze'ev	86.12	129.72	197.39	34%	52%
Hashmonaim	17.29	42.94	53.88	60%	25%
Immanuel	36.67	40.10	63.90	9%	59%
Karnei Shomron	78.85	112.60	154.95	30%	38%
Kfar Etzion	7.27	39.93	49.87	82%	25%
Kfar Tapuah	10.61	17.21	26.73	38%	55%
Kiryat Netafim	2.00	11.86	18.04	83%	52%
Kochav Ya'akov	16.21	50.70	84.53	68%	67%
Ma'ale Adumim	191.12	413.90	447.98	54%	8%
Matityahu	14.28	30.66	44.94	53%	47%
Migdal Oz	10.27	18.88	20.55	46%	9%
Modi'in Ilit	40.43	249.26	350.58	84%	41%
Na'ale	3.93	38.01	68.75	90%	81%
Neve Daniel	9.94	34.75	54.46	71%	57%

Nili	19.55	34.25	58.31	43%	70%
Nofim	26.81	29.74	33.75	10%	13%
Oranit	64.74	132.31	161.30	51%	22%
Psagot	13.20	24.39	28.65	46%	17%
Rosh Tzurim	8.69	23.72	30.57	63%	29%
Sha'arei Tikva	42.52	80.36	85.62	47%	7%
Shavei Shomron	14.12	18.88	21.30	25%	13%
Tzofim	14.53	27.48	35.00	47%	27%
Yakir	21.63	32.08	46.94	33%	46%

4.4 PREDICTIVE MODELLING OF SETTLEMENTS

4.4.1 CA-MARKOV TRANSITION MATRIX VALIDATION

To predict future land use, the LCM uses Markov-chain probabilities to establish the likelihood of a class transitioning to another (Table 8). The probability of a land use class transitioning to a settlement pixel is generally low, however these probabilities roughly double from 2024-2034, such as for farmland, which increases from 0.014 to 0.029. This pattern repeats in 2054, where farm transition probability to settlement increases from 0.029 to 0.061. The land use class with the highest probability of transition is bare land, followed by vegetation, then farmland.

Table 8. Transition Area Matrices for CA-Markov Transition Probabilities, for 2024, 2034, and 2054.

2024					
	farm	bare	vegetation	built	settlement
farm	0.880	0.025	0.056	0.025	0.014
bare	0.031	0.846	0.035	0.032	0.057
vegetation	0.107	0.030	0.820	0.019	0.024
built	0.051	0.055	0.011	0.883	0.000
settlement	0.000	0.000	0.000	0.000	1.000
2034					
	farm	bare	vegetation	built	settlement
farm	0.778	0.047	0.099	0.047	0.029
bare	0.058	0.715	0.063	0.057	0.107
vegetation	0.190	0.055	0.673	0.036	0.046
built	0.096	0.100	0.023	0.781	0.000
settlement	0.000	0.000	0.000	0.000	1.000
2054					
	farm	bare	vegetation	built	settlement
farm	0.632	0.080	0.148	0.080	0.061
bare	0.104	0.523	0.094	0.091	0.188

vegetation	0.282	0.089	0.476	0.064	0.089
built	0.160	0.156	0.049	0.636	0.000
settlement	0.000	0.000	0.000	0.000	1.000

4.4.2 SETTLEMENT AREA PREDICTION IN 2034 AND 2054 WITH SCENARIOS

Settlement areas are predicted for BAU, low-growth/high constraint, and high-growth/low-constraint scenarios for 2034 and 2054 (Table 9) (Figure 4-7). The area of settlements is predicted to increase from 3,636 hectares in 2024 to 4,210 hectares in 2034, under a BAU scenario. By 2054, settlements are expected to increase to 5,532 hectares, representing 5.16% of the study area. In the low-growth/high-constraint scenario, growth is smaller at 3,929 ha, a 6.67% decrease in growth. In 2054, the low growth scenario has a smaller growth at 4,986 ha, representing a 9.87% decrease in growth compared to BAU. In contrast, the high-growth/low-constraint scenario shows settlement growth at 5,089 ha in 2034, which is a 20,89% increase from the BAU scenario. Further, in 2054, the predicted ha is 7,238 for settlements, which is 30.88% higher than the BAU scenario.

The transition of the other land classes assessed in this study to settlement are also shown (Table 9). Farmland shows the consistently highest transition to settlement, due to it being the dominant land class in the study area. This also aligns with the decreasing trend of farmland illustrated in LULC change from 1994 – 2024.

Table 9. Predicted area of settlements for BAU, Low-growth/High-constraint, and High-growth/Low-constraint scenarios, expressed in hectares (ha) and % of study area. Area of transitions to settlement for each land class are listed under.

	2034						2054					
	BAU	%	LOW	%	HIGH	%	BAU	%	LOW	%	HIGH	%
Settle-ment area	4,174	3.93	3,912	3.67	4,994	4.75	5,429	5.16	4,933	4.65	7,015	6.75
Transition to Settlement												
Farm	477	0.45	379	0.35	821	0.77	1,058	0.99	837	0.78	1,776	1.66
Bare	195	0.18	160	0.15	359	0.33	411	0.38	328	0.31	772	0.72
Vegetation	280	0.26	212	0.20	484	0.45	587	0.55	447	0.42	1,009	0.94

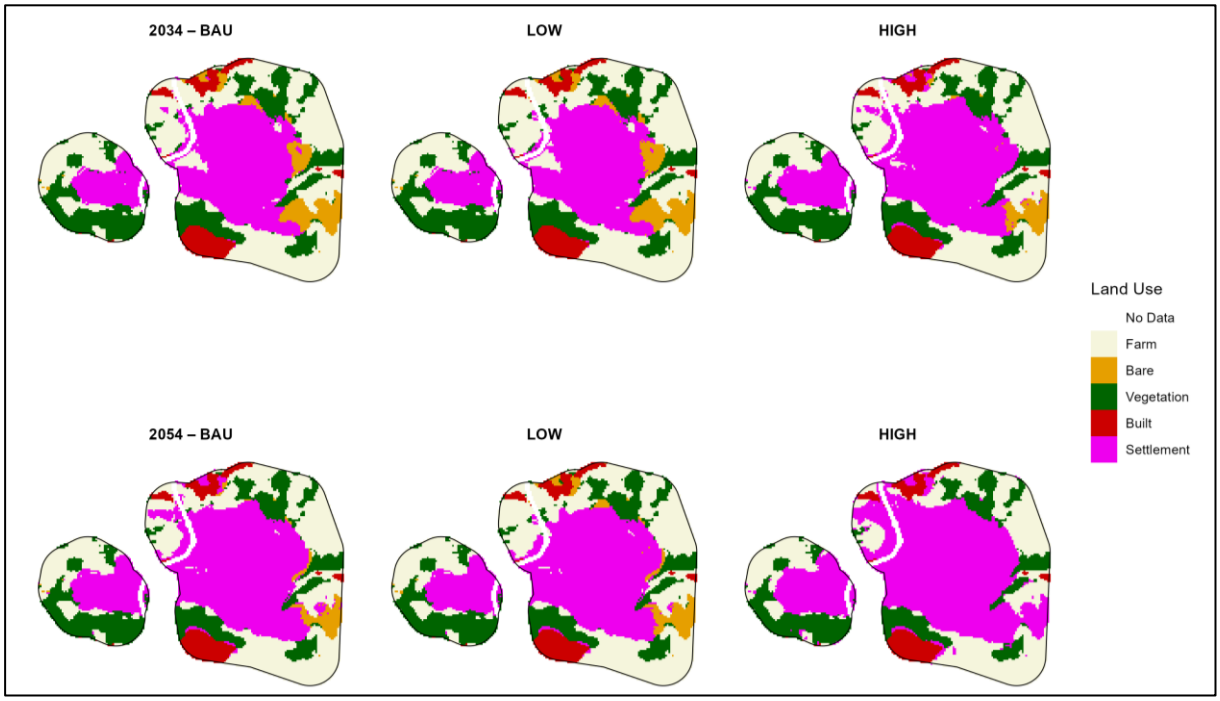

Figure 4-7. Scenario predictions for BAU (left), Low-growth/High-constraint (middle), and High-growth/Low-constraint (right) for the example settlement of Modi'in Illit, for 2034 (top) and 2054 (bottom).

4.4.3 Directionality and Intensity of Growth with Predictions

Directionality and intensity of settlement growth were calculated for the periods of 1994 – 2024, and 2024 – 2054 (Figure 4-8). The intensity of settlement growth for 1994 – 2024 peaks at 600 – 1,000 growth pixels/km^2, whereas for 2024 – 2054 it is lower at 300 – 500 growth pixels/km^2. Further, for 1994 – 2024, settlement growth is more clustered around the city of Jerusalem, whereas settlements farther away show less intensity. This is also evidenced by the rose diagram on the top right, where settlement growth is most in the south of the study area, closer to the major city of Jerusalem.

In contrast, the 2024 – 2054 shows less intensified settlement growth overall, and growth is more evenly split across the study area. This is evidenced by more red colouring in all settlements across the study area, as well as in the rose diagram, where petals are generally larger than in 1994 – 2024.

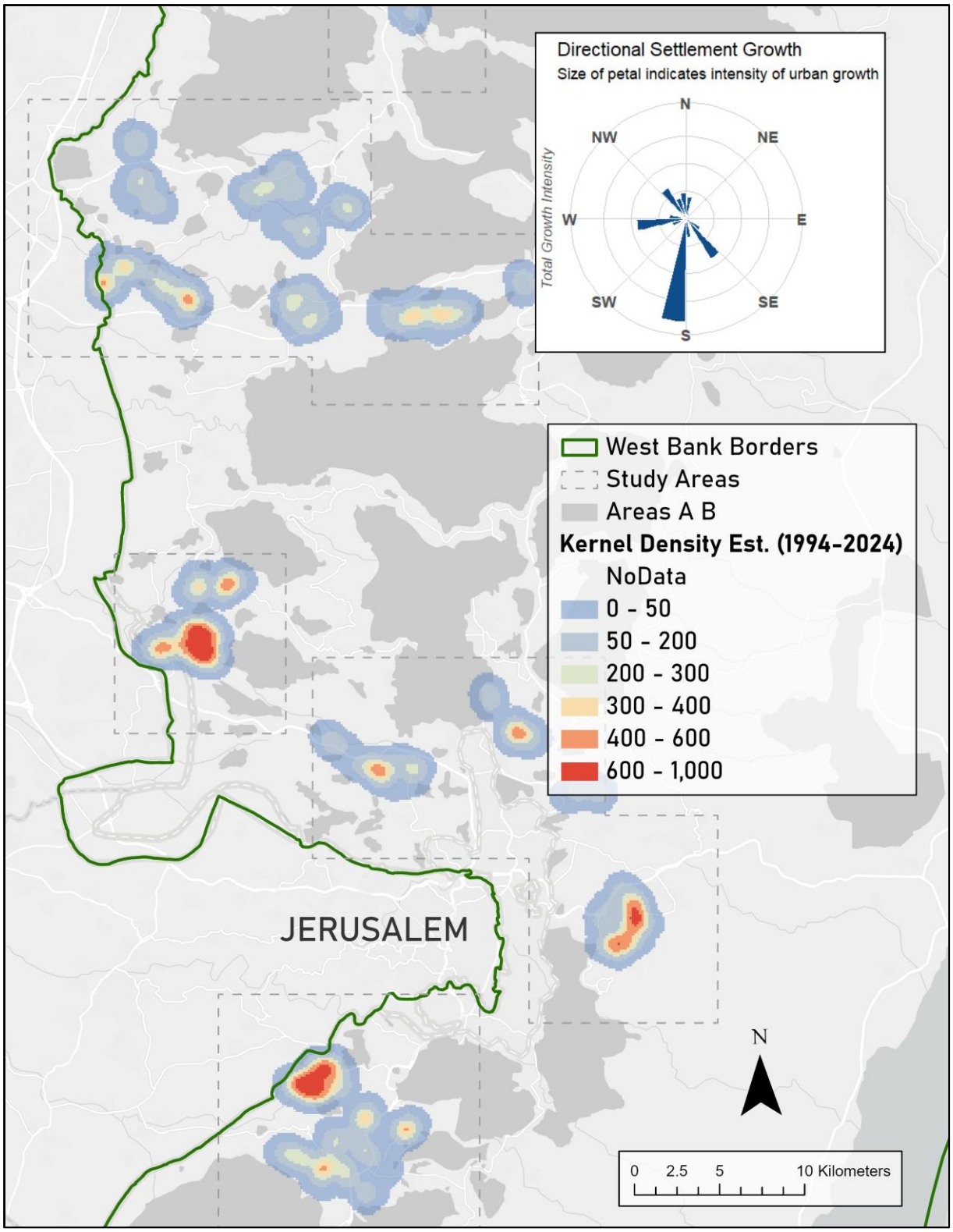
Directional Settlement Growth
Size of petal indicates intensity of urban growth
N
NE
E
SE
S
SW
W
NW
Total Growth Intensity
West Bank Borders
Study Areas
Areas A B
Kernel Density Est. (1994-2024)
NoData
0 - 50
50 - 200
200 - 300
300 - 400
400 - 600
600 - 1,000
JERUSALEM
N
0 2.5 5 10 Kilometers

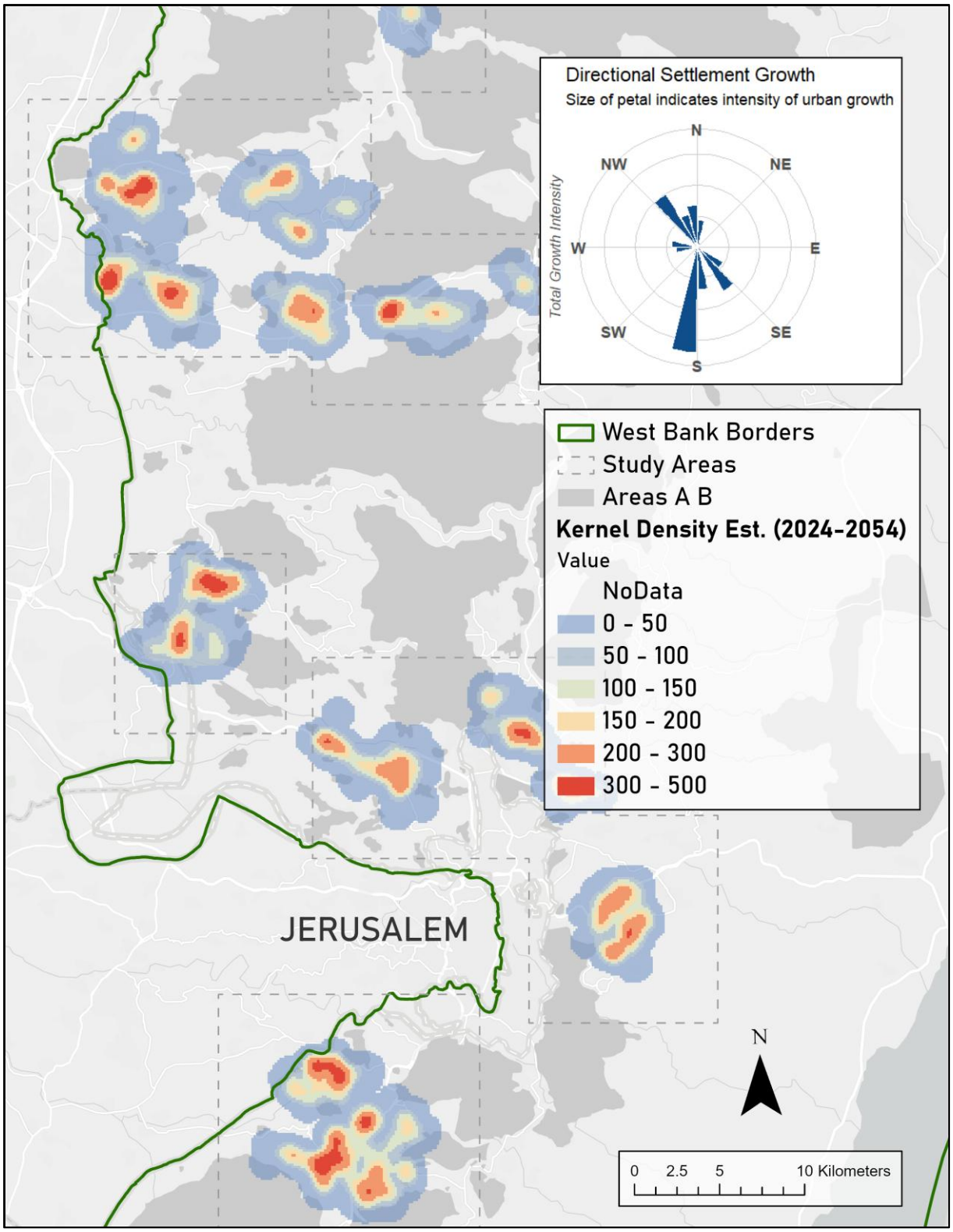

Figure 4-8. Top image: intensity of settlement growth from 1994 - 2024. Bottom image: intensity of settlement growth from 2024 – 2054. Units represent magnitude of settlement growth per square kilometre (growth pixel/km2). Red areas show higher intensity, whereas low areas are in beige/light blue. The rose diagram is shown on the top-right corner of both images. The size/length of the petal indicates the intensity

of growth in that cardinal direction. Note that image legends are different for 1994 – 2024, and 2024 – 2054, with 2024 – 2054 showing less intensity overall.

4.4.4 EXPLANATORY POWER OF DRIVERS

The explanatory power of the selected drivers was calculated using the LCM in Terrset (Table 10). The 1994 settlement area has the most explanatory power for modelling the transition to settlement for bare, farm, and vegetation land from 1994 to 2014, at a very strong 0.90. This may be because of the autocorrelative effect of settlement growth. After this, distance to roads was also very important, as well as distance to railways. Distance to Areas A, B and the separation wall, as well as distance to major cities and towns, had equally strong explanatory power at 0.60. Elevation, distance to waterways, and slope had the least explanatory power in the dataset, although they were kept in the model to the correlative effect of drivers, where their combination with other drivers aids the model's predictive power (Eastman et al., 2024).

Table 10. Drivers and their explanatory ratio (ER) for modelling land use transitions to settlement land, for transitions from 1994 - 2014. Sorted by average value.

Driver	Explanatory Ratio (ER)			
	bare	farm	vegetation	Average
distance to 1994 settlement area	0.90	0.90	0.90	0.90
distance to roads	0.72	0.70	0.65	0.69
distance to railways	0.70	0.54	0.58	0.61
distance to Areas A, B; Separation Wall	0.57	0.60	0.64	0.60
distance to major cities	0.60	0.56	0.63	0.60
distance to towns	0.65	0.49	0.61	0.59
elevation	0.48	0.41	0.52	0.47
distance to waterways	0.45	0.19	0.28	0.31
slope	0.20	0.23	0.27	0.23

4.4.5 DECISIONFOREST SUBMODEL PERFORMANCE

Key parameters and performance metrics for the DF were calculated using TerrSet LCM (Table 11). All sub models used the same parameters for the DF model at 500 trees and 4 variables selected at split. These parameters gave the highest accuracy

and skill, while optimizing runtime of the model. Sample sizes differed for the DF model, depending on the number of transitions that occurred within the dataset. The farm transition has the highest sample size due to being the dominant class within the dataset, while vegetation has the lowest. Overall OOB accuracy and skill were high, at over 94% accuracy and 0.89 skill for all sub models; showing that the sub models could predict transition to settlement better than random chance. The model also outputs accuracy levels, holding different driver variables constant. The biggest drops in accuracy are seen in holding 1994 settlement area constant, illustrating its predictive power in the model due to spatial autocorrelative effects.

Table 11. Key parameters and performance for DecisionForest sub-modelling of land use transitions.

Variable	bare	farm	vegetation
Number of trees		500	
Number of variables selected at split		4	
Sample size	5,219	8,430	3,485
OOB Accuracy	97.00	94.77	94.60
OOB Skill	0.94	0.90	0.89
Acc. holding barriers constant	96.91	94.67	94.61
Acc holding cities constant	96.91	94.58	94.46
Acc. holding elevation constant	96.87	94.6	94.52
Acc. holding railways constant	96.87	94.55	94.43
Acc. holding roads constant	97.12	94.83	94.76
Acc. holding 1994 settlement area constant	96.88	93.41	93.73
Acc. holding slope constant	97.1	94.98	94.79
Acc. holding towns constant	96.76	94.39	94.24
Acc. holding waterways constant	96.9	94.42	94.44

4.4.6 VALIDATION OF PREDICTIVE MODEL

To validate the predictive power of our model, the predicted map of 2024, under the BAU scenario as it reflects reality the most, was validated against the actual 2024 map to calculate the FoM, quantity disagreement, allocation disagreement, and overall accuracy over the settlement space (Table 12). The FoM for predicted settlement change is 22.05%, meaning that 22.05% of predicted settlement expansion matched explicitly with actual settlement expansion in 2024. This metric does not include settlement pixels that were the same between 2014 and 2024. Breaking down the FoM metric; 3,188 pixels of predicted expansion occurred in the actual map (hits), 5,965 pixels of actual settlement expansion were missed (misses),

and 5,307 pixels of predicted settlement expansion were misallocated (false alarms). Because more misses than false alarms were generated, the model was slightly under predictive of overall settlement growth.

Further, we achieved a quantity disagreement of 1.37%, showing excellent agreement with the amount of settlement growth that occurred, but an allocation disagreement of 22.07%. This means the quantity of growth was well predicted, but the location of where this growth occurred was erroneous (Figure 4-8). Many false alarms are evenly spread around the perimeters of the settlements, while misses appear to occur in smaller, more homogenous clusters (Figure 4-8). It appears the model predicts even growth around the settlement, while actual growth occurs in clusters. Including pixels of persistence, our predicted settlement model aligned 76.57% with actual settlements in 2024.

Table 12. Validation metrics of predicted pixels of settlements for 2024 using 1994-2014 transitions, compared with actual 2024 settlement pixels.

Validation Metrics	Value
Figure of Merit (FoM) (%)	22.05
Hits	3,188
Misses	5,965
False Alarms	5,307
Quantity Disagreement (%)	1.37
Allocation Disagreement (%)	22.07
Total Disagreement (%)	23.43
Accuracy within Settlement Space (%)	76.57

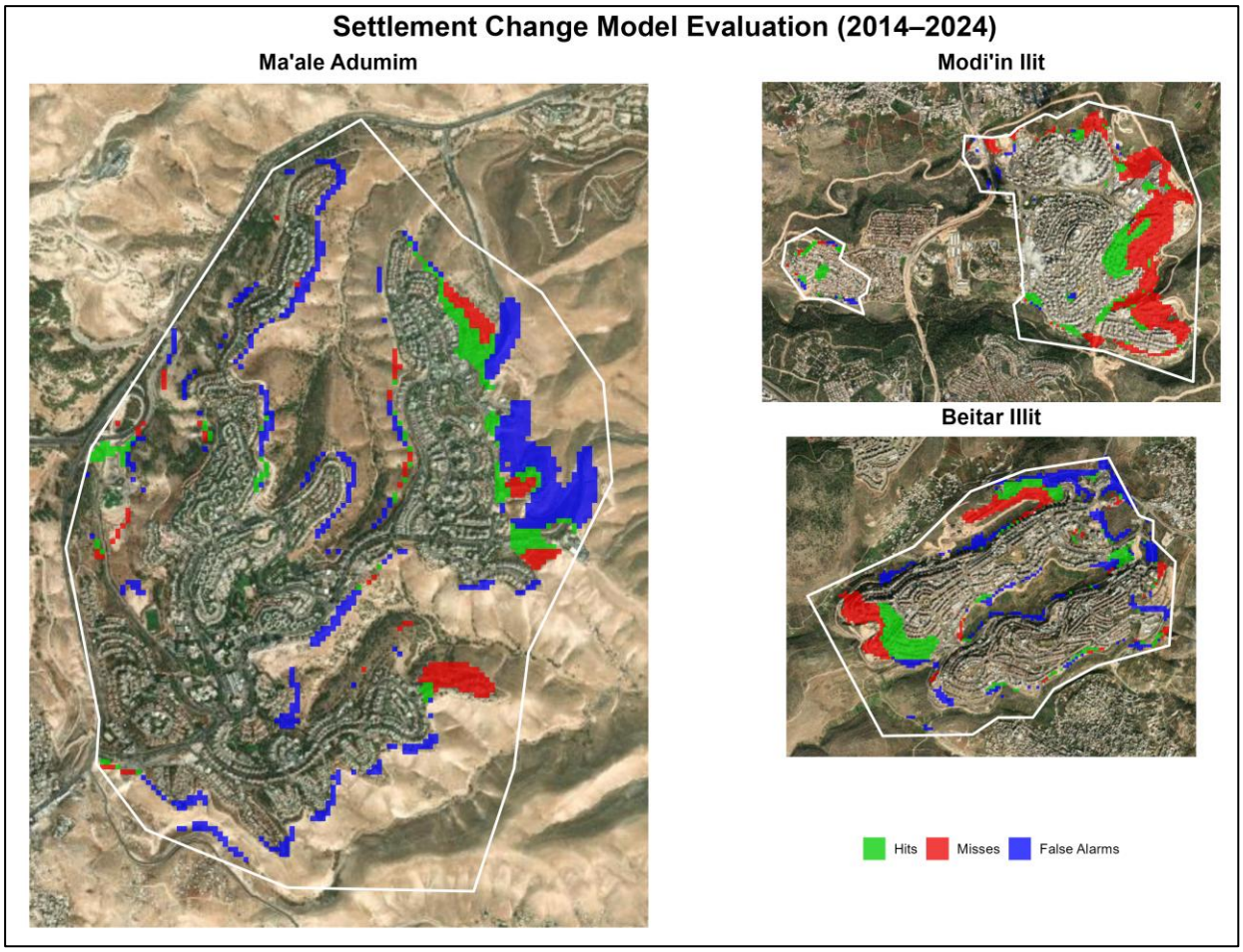

Figure 4-9. Map of predictive map validation in major settlements: Ma'ale Adumim (left), Modi'in Illit (top right), Beitar Illit (middle right). Green areas are pixels of settlement expansion correctly predicted (Hits), Red are pixels of actual settlement expansion that were not predicted (Misses), and Blue are pixels of predicted settlement growth that did not occur in the actual image (False Alarms).

5 DISCUSSION

5.1 ALIGNMENT WITH RESEARCH QUESTIONS

The first goal of our study was to establish how settlements and their surrounding land changed over time. In our study of urban built-up growth in settlements in the West Bank, we used satellite imagery and the random forest algorithm to evaluate LULC changes in select areas in 1994, 2014, and 2024. We found that farmland has decreased from 68,852 to 49,456 hectares from 1994 - 2024, while built and settlement land grew rapidly over the same time. Settlement land showed the highest

relative growth of all land classes in the study, expanding from 1,405 to 3,636 hectares. We also saw that losses in farmland and bare land contributed the most to settlement expansion. The average settlement grew horizontally by 49% from 1994 – 2014, then 34% from 2014 – 2024.

Our second goal was to establish how settlements will grow in the future, according to different scenarios. Upon examination of individual settlement extents, we found that the median CAGR for settlements in our study area is 2.84% from 1994 – 2024, with a lower 25%-quartile of 2.27% and upper 75%-quartile of 4.62%. We then used Decision Forest sub modeling in LCM to predict CA-Markov transition matrices, with the lower and upper quartiles informing scenarios of low and high growth, to predict growth in settlements in 2034 and 2054. We found that settlement growth ranged from 3,929 ha in a low-growth scenario, 4,210 ha in BAU, and 5,089 for high-growth for 2034, For 2054, these numbers were 4,896, 5,532, and 7,238 ha for low, BAU, and high growth scenarios, respectively.

The final goal of the research was to establish where settlements were growing the most, and the subsequent impact of the expansion on surrounding land uses. We determined that from 1994 – 2024, settlement growth was most clustered to the south of the dataset, nearby the major city of Jerusalem. From 2024 – 2054, the model predicts more even growth across the study area. Finally, we found that farmland will be the most impacted by settlement expansion, followed by bare and vegetated land.

5.2 Comparison of Results

The finding of the research implies severe consequences for rapid urban growth in settlements in the West Bank. The expansion of settlements has detrimental impacts for Palestinian communities, such as the further constriction of space and restriction of movement (Ghodieh, 2020). Settlements and Palestinian communities frequently come into violent contact, especially as settlements encroach on agricultural land and vineyards (UNHRC, 2013). The area of influence of a settlement is far greater than its actual physical extent (Ghodieh, 2020). Constrictions must be set on settlement land encroachment in areas of high agricultural and water suitability.

Other studies within or near the study area also have reported on similar LULC trends occurring in the West Bank and Gaza strip. Ghodieh (2020) uses aerial photography and medium-resolution satellite imagery to visually identify Palestinian built-up lands and settlements, as well as a Maximum Likelihood Classifier to classify LULC in the entirety of the West Bank. They found that Palestinian built-up communities grew by 176% from 1997 to 2016, and that settlements grew by 77.56% over the same time span. They confirm the trend of built up expansion at the cost of agricultural land, with 63% of total urban expansion occurring on agricultural land (Ghodieh, 2020). Nazer et al., (2019) use GIS and FRAGSTATS analysis to explore landscape change in Ramallah city, West Bank, Palestine. They found an increase in built-up area by 85%, at the expense of permanent agriculture trees, arable land, and open tree plantation (Nazer et al., 2019). Both authors of these papers found that the expansion of settlement impacted the city-building of Palestinian areas, leading to densification due to political and security restrictions (Ghodieh, 2020; Nazer et al., 2019). Attaalah (2018) models LULC change using CA-Markov in IDRISI software in the Gaza strip. They find that built-up area increases by 15.83 percentage points of the total area, while agricultural land and soil decrease by 4.46 and 11.37 percentage points, respectively (Attaallah, 2018).

Further, the findings of the directionality and intensity of settlement growth are supported by the work of Allegra and Maggor (2022) and Schwake (2020). Drivers of historical settlement growth has diverted from the dispersed, wide-spread intentions of control to modern neo-capitalist, market-based urban growth to support a growing metropolitan base in major cities (Schwake, 2020).

We validated the results of our predictions by comparing our predicted map of settlement extent in 2024 to the map of ‘actual’ 2024 settlement extent classified by our random forest. I calculated a value of 22.05% FoM, and a 1.37% quantity disagreement and 22.07% allocation disagreement. We also found an accuracy within the ‘settlement’ space of 76.57%. To the knowledge of the author, no other studies report the accuracy of the category ‘space’ and rather report overall accuracy. This may be due to the tendency of urban growth prediction studies to predict multiple categories of land use, instead of a comparison with just a single category (Badshah et al., 2024; Hanoon et al., 2023; Singh et al., 2022). Further, as

stated earlier in this study, many research papers tend to report overall accuracy and kappa co-efficient as the main metrics of validation, although these metrics have been harshly criticized and are not informative of the actual quality of the prediction (Pontius Jr & Millones, 2011).

Figure of Merit is not as widely reported but serves as a valuable metric in quantifying prediction accuracy (Pontius Jr et al., 2025; Varga et al., 2019). Other studies report FoM to various degrees. Pontius (2025) states that the median value of FoM is usually found to be 0.2, but does not offer qualifying statements of 0.2 being acceptable or not – rather stating it is up to the intents and research questions of the author (Pontius Jr et al., 2025). Tang et al., (2024) report a FoM of 0.4303 for a prediction in 2010, and 0.3764 in 2020 using a GSA-CA method in predicting urban growth in a desert area. Xiacong et al., (2022) model urban growth in Toronto with a A-VCA model and achieve a FoM of 0.283. Zhang et al., (2023) report a range of FoM values for urban growth prediction in their study area, from 0.058 to 0.122. Quantity (q_g) and allocation disagreement (α_g) are also metrics that are not as commonly reported but valuable in understanding differences between predicted and reference maps (Pontius Jr et al., 2025). Zhang et al., (2023) report q_g between 0.7 and 8.33%, and $\alpha_g$between 0.94 and 2.06%. Mesta et al., (2022) model urban growth in Kathmandu Valley and find $q_g$and α_g of 5.1% and 7.3%. Finally, Pickard et al., (2017) compared model performance using these metrics, and found q_g ranged from 0.3 – 10.60%, and α_g 8.4 – 18.56% for their study area.

From the literature, we can see that our classification results align well with other studies, and our predictive model's metrics falls within a suitable range. However, the allocation disagreement is high. This may be due to the prioritization of autocorrelative growth in settlements, where we observed that actual settlement growth occurred in clusters. This behaviour may be improved with more sophisticated drivers, such as the incorporation of Israeli settlement planning documents to the prediction.

5.3 Limitations and Errors Analysis

Many limitations are apparent within this analysis, that must be addressed. Firstly, there exists a problem of ground-truth data availability for the RF model. The reference data used was generated by the Palestinian Ministry of Land for 2016 only and hence did not directly relate to our study dates of 1994, 2014, or 2024. This limitation is most apparent in the discrimination of vegetated and farmland, which we acknowledged have significant pixel mixing due to the nature of farm systems in the West Bank. The LULC map would be much improved with the verification of an expert with local knowledge of the area, or using alternative, verified sources for LULC mapping, although these resources were not publicly available to the knowledge of the author. Due to the limitations of the reference data, the accuracy of the RF classification can not be said to be fully representative of the ground-truth, particularly for 1994, where neither strong reference data nor very high-resolution satellite data is available for verification. Secondly, the removal of the bands was performed using the same CV in the random forest, potentially optimistically biasing the results of the analysis.

The errors generated during the RF classification and their propagation throughout the results should also be discussed. We observe the following trends: the producer's accuracy for farmland is consistently higher than the user's accuracy by about 10% for all years, the user's accuracy for vegetation is consistently higher than the producers accuracy by roughly 15%, and the user's accuracy for built land is 10% higher than its producers accuracy in 1994 only, and the UA is higher in 1994 than compared to 2014 and 2024. We can then make the following conclusions, based on the proportions of each error: firstly, our LULC maps consistently overpredict farmlands for all years, as we commit more commission than omission error. Secondly, and inversely, we are too strict in our classification of vegetation, leading to an underrepresentation of vegetated land in our maps. Thirdly, and most importantly, we likely underpredict the quantity of built land in 1994 but slightly overpredict it in 2014 (and prediction errors are stable in 2024). Further, because our UA is higher in 1994 than the latter years, we can say we were more liberal in prediction for 2014 and 2024. These errors illustrate that we potentially overstate the quantity of built/settlement land growth from 1994 – 2024. This then propagates into

our predictions, where projected future built/settlement land growth may be similarly overzealous.

The trend of potential overstatement of built/settlement growth was also analyzed through the application of the temporal filtering rules (Table 4), where we applied several transition rules based on assumptions of unlikely transitions to settlement land, as well as transitions to and from vegetation and farmland. We see that the greatest proportion of settlement land affected was in 1994, where we removed settlement pixels if they did not exist in 2014 or 2024, changing about 9.0% of the pixels in that category, but only 0.14% of pixels in the entire study area (Table 4). Comparing the confusion matrices from before and after temporal filtering (Appendix F), we can see that temporal filtering had a very small to zero impact on the potential overstatement of settlement land, as the total percentage of pixels changed in 1994 was too minimal to impact the confusion matrix meaningfully.

An important question to ask is whether the thesis was supplemented through the RF classification, or if it would have benefitted from using an automatically generated LULC maps such as the GLC-FCS30D, which is a publicly available dataset generated worldwide across a long timespan. The GLC-FCS30D is a popular option for researchers in data-scarce regions, where reputable, robust maps of LULC are not as readily available (Tang et al., 2024). We compared the results of the GLC-FCS30D for the dates of 1995, 2014, and 2022, as these were the closest dates with data available to our study dates, to see how differently the methods defined LULC in the study area (Appendix E). We observe that the GLC amplifies problems in the overstatement of farmland, where it reports 6,633 ha more farmland than RF, and understates built land in 1994: reporting 4,557 ha to the RF model's 9,940 ha. Further, the GLC map shows very limited urban growth from 2014-2022 at 543 ha, or 68 ha annually, compared to the astronomically higher 736 ha annually from 1994 to 2014. Our RF model shows built land grew by 383 ha annually between 2014-2024, compared to a more reasonable 467 ha annual growth from 1994 – 2014. Further, the reported mean accuracy for the GLC-FCS30D model is 82.5%, while we report 89.8% (X. Zhang et al., 2024). We can then confidently say our model does outperform the use of automatically generated datasets such as GLC.

Another limitation of the model is that it serves as a good predictor of horizontal expansion of settlements that can be seen from a satellite. The model does not predict where entirely new settlement may be constructed in Area C, nor does it predict vertical growth of settlements, or where settlements may be increasing in density. Future work to predict new settlement locations may be valuable research.

5.4 Future Research

The prediction model could be improved with the inclusion of an additional year between 1994 and 2014, such as 2004. Multiple other studies used a four-time-step process to model land use transitions, using the extra year to help further validate predictions. To better capture current settlement trends, a date between 2014 – 2024 can also be considered.

There are many avenues for future research that this model lays the foundation for. Urban built-up prediction has evolved past simple CA-Markov into exciting new models that may have better predictive ability, such as Deep Neural Networks, XGBoost (Tahmi et al., 2025), and Gravitational-Search-Algorithm-CA (Tang et al., 2024), which all obtained excellent results in urban built up prediction. Additionally, further comparative studies of the performance of different predictive models like SLEUTH, FLUS, MOLUSCE, and TerrSet LCM can prove valuable for researchers wishing to select the best model for their use case.

Alternative methodological approaches to cellular automata and Markov models should also be considered in evaluating urban settlement growth, such as Dynamic Time Warping (DTW), Hidden Markov, and Deep-Learning with CNN (convolutional neural network)/ U-Net. Torchiana et al., propose a Hidden Markov Model (HMM) to correct transition rates of different land use classes that does not require any ground-truth data (Torchiana et al., 2025). Zhang, Yanghua & Zhao, Hu use two-year time-series Landsat images to track pixel trajectories in urban areas. With DTW, they extract accuracies of 71% for the whole dataset, and find transitions in mixed-pixel areas like agriculture -> forest were detected by the method (Y. Zhang & Zhao, 2020). Finally, a CNN-LSTM model was employed in Riyadh, which used unsupervised machine learning to predict urban growth to greater accuracies than other models (Boulila et al., 2021).

6 CONCLUSION

The work presented in this thesis helps address the lack of systematic, long-term, and automated approaches to LULC modelling, particularly in Israeli settlements, in the West Bank. Using multi-temporal satellite imagery, supervised random forest modelling, and ML-assisted CA-Markov modelling using LCM, the thesis aimed to quantify historical satellite growth and predict future expansion under differing scenarios of settlement growth.

Firstly, we aimed to quantify how the spatial extent and surrounding land of settlements changed over time, using publicly available satellite imagery and RF classification. We found that settlements more than doubled in area from 1994 – 2024, with primary contributions from bare and agricultural land. The accuracies of the classification were robust, although 1994 built land was generally underestimated, while 2014 and 2024 was relatively overestimated. This confirms existing scholarship that settlement growth has been occurring rapidly in the West Bank, at the expense of farmed land and land cleared for construction.

Secondly, we successfully simulate future growth of settlements to 2034 and 2054, using historical transition data. We find that, in the comparison of BAU, low-growth, and high-growth scenarios, that high growth will have severely more damaging impacts than other scenarios. Further, we see that from the drivers of urban growth, existing settlement area from 1994 and roads were the best for predicting future growth. Validation of the 2024 predicted area with our 2024 LULC shows moderate agreement, although the model would greatly benefit from more spatial knowledge due to its high allocation error. The modelled growth maps of the settlements can be used to supplement Palestinian government policy and identify areas at risk of future expansion.

Finally, we ask which areas the settlements will grow most intensely, and what the impact of that growth will be. Directional and intensity modelling indicate that historical settlement growth is more clustered around the metropolitan area of Jerusalem, while future growth is predicted more evenly across the study area. This confirms existing research on settlement expansion from Israeli suburbanization in

the region. We also see that settlements will expand on agricultural areas the most, then bare and vegetated land.

Despite the robust results, several major limitations hamper the significance of the results. Most importantly, the RF classification was performed by someone not knowledgeable of the study area, and existing ground-truth data was very limited. The study would greatly benefit from local knowledge, or alternative methods that lessen the impact of poor ground-truth availability, like HMM or DTW methods. Secondly, the Markov model assumes stationarity, although the study area is extremely politically volatile. While the scenarios aid in addressing this limitation, they do not fully encompass major political decisions that may occur in the future. Third, the model lacked spatial knowledge, which would be aided through master plan documents and socio-economic data, although this data was not available to the author's knowledge. Future work should aim to incorporate these variables. Research was limited to a smaller study area as a representative sample of the West Bank. Future work should aim to incorporate the entirety of settlements and outposts in the West Bank.

This thesis contributes a novel, automated, and spatially explicit framework for analysing and predicting Israeli settlement expansion in the West Bank over a 30-year period. Through RF classification and ML-assisted CA-Markov scenario modelling, the study bridges RS methodology with politically contested land transition analysis. The results demonstrate not only the current and future trajectory of settlement growth, but also the capacity of geospatial technologies to provide transparent and reproducible research in contested, data-scarce areas. However, this thesis fits into one piece of a larger puzzle of Israeli expansionism in the West Bank and Palestine. Far more research is needed to fully understand the impacts of settlements, as well as aid policymakers in future spatial decision-making processes. As land transformation continues to shape humanitarian and geopolitical realities in the West Bank, spatial modelling offers an essential tool for evidence-based understanding and informed decision-making.

BIBLIOGRAPHICAL REFERENCES

Abbas, D. Z., Khan, D. R., & Khan, D. S. R. (2024). Conceptualizing Human Rights Violations in Israel-Hamas War: Analyzing Gaza Conflict (October 2023-November 2024). *Contemporary Journal of Social Science Review*, *2*(04), Article 04.

Abdelkarim, A. (2025). Monitoring and forecasting of land use/land cover (LULC) in Al-Hassa Oasis, Saudi Arabia based on the integration of the Cellular Automata (CA) and the Cellular Automata-Markov Model (CA-Markov). *Geology, Ecology, and Landscapes*, *9*(1), 13–44. https://doi.org/10.1080/24749508.2022.2163741

Abuelaish, B. (2018). Urban Land Use Change Analysis and Modeling: A Case Study of the Gaza Strip. In M. T. Camacho Olmedo, M. Paegelow, J.-F. Mas, & F. Escobar (Eds.), *Geomatic Approaches for Modeling Land Change Scenarios* (pp. 271–291). Springer International Publishing. https://doi.org/10.1007/978-3-319-60801-3_13

Abuelaish, B., & Olmedo, M. T. C. (2016). Scenario of land use and land cover change in the Gaza Strip using remote sensing and GIS models. *Arabian Journal of Geosciences*, *9*(4), 274. https://doi.org/10.1007/s12517-015-2292-7

Al-Dousari, A. E., Mishra, A., & Singh, S. (2023). Land use land cover change detection and urban sprawl prediction for Kuwait metropolitan region, using multi-layer perceptron neural networks (MLPNN). *The Egyptian Journal of Remote Sensing and Space Science*, *26*(2), 381–392. https://doi.org/10.1016/j.ejrs.2023.05.003

Allegra, M., & Maggor, E. (2022). The metropolitanization of Israel's settlement policy: The colonization of the West Bank as a strategy of spatial restructuring. *Political Geography*, *92*, 102513. https://doi.org/10.1016/j.polgeo.2021.102513

Alqadhi, S., Mallick, J., Balha, A., Bindajam, A., Singh, C. K., & Hoa, P. V. (2021). Spatial and decadal prediction of land use/land cover using multi-layer perceptron-neural network (MLP-NN) algorithm for a semi-arid region of Asir, Saudi Arabia. *Earth Science Informatics*, *14*(3), 1547–1562. https://doi.org/10.1007/s12145-021-00633-2

Area C | B'Tselem. (2024, September 5). https://www.btselem.org/topic/area_c

Ashwini, K., & Sil, B. S. (2022). Impacts of Land Use and Land Cover Changes on Land Surface Temperature over Cachar Region, Northeast India—A Case Study. *Sustainability*, *14*(21). https://doi.org/10.3390/su142114087

Asif, M., Kazmi, J. H., Tariq, A., Zhao, N., Guluzade, R., Soufan, W., Almutairi, K. F., Sabagh, A. E., & Aslam, M. (2023). Modelling of land use and land cover changes and prediction using CA-Markov and Random Forest. *Geocarto International*, *38*(1), 2210532. https://doi.org/10.1080/10106049.2023.2210532

Attaallah, H. (2018). Modeling of built-up lands expansion in Gaza Strip, Palestine using Landsat data and CA-Markov model. *IOP Conference Series: Earth and Environmental Science*, *169*(1), 012035. https://doi.org/10.1088/1755-1315/169/1/012035

Badshah, M. T., Hussain, K., Rehman, A. U., Mehmood, K., Muhammad, B., Wiarta, R., Silamon, R. F., Khan, M. A., & Meng, J. (2024). The role of random forest and Markov chain models in understanding metropolitan urban growth trajectory. *Frontiers in Forests and Global Change*, *7*. https://doi.org/10.3389/ffgc.2024.1345047

Bashyal, S., Gautam, J., Poudel, P., & Subedi, B. (2024). Land Use Land Cover Change Prediction of Tansen Municipality Using Multi-Layer Perceptron-Markov Chain (MLP-MC) Model. *Forestry: Journal of Institute of Forestry, Nepal*, *21*, 66–82. https://doi.org/10.3126/forestry.v21i1.79686

Belgiu, M., & Drăguţ, L. (2016). Random forest in remote sensing: A review of applications and future directions. *ISPRS Journal of Photogrammetry and Remote Sensing*, *114*, 24–31. https://doi.org/10.1016/j.isprsjprs.2016.01.011

Boulila, W., Ghandorh, H., Khan, M. A., Ahmed, F., & Ahmad, J. (2021). A novel CNN-LSTM-based approach to predict urban expansion. *Ecological Informatics*, *64*, 101325. https://doi.org/10.1016/j.ecoinf.2021.101325

Breiman, L., Friedman, J., Olshen, R. A., & Stone, C. J. (2017). *Classification and Regression Trees*. Chapman and Hall/CRC. https://doi.org/10.1201/9781315139470

Çağlıyan, A., & Dağlı, D. (2022). Monitoring Land Use Land Cover Changes and Modelling of Urban Growth Using a Future Land Use Simulation Model (FLUS) in Diyarbakır, Turkey. *Sustainability*, *14*(15). https://doi.org/10.3390/su14159180

Chouhan, R. L., & Shekhawat, H. S. (2025). A Hybrid Approach to Predicting Land Use/Land Cover Change: Integrating Object-Based Detection with Machine Learning. *ELECTRICA*, *25*(1), 1–10. https://doi.org/10.5152/electrica.2025.24181

Demir, S., & Sahin, E. K. (2023). Random Forest Importance-Based Feature Ranking and Subset Selection for Slope Stability Assessment using the Ranger Implementation. *Avrupa Bilim ve Teknoloji Dergisi*, (48), 23–28. https://doi.org/10.31590/ejosat.1254337

Dey, N. N., Al Rakib, A., Kafy, A.-A., & Raikwar, V. (2021). Geospatial modelling of changes in land use/land cover dynamics using Multi-layer Perceptron Markov chain model in Rajshahi City, Bangladesh. *Environmental Challenges*, *4*, 100148. https://doi.org/10.1016/j.envc.2021.100148

Duan, X., Haseeb, M., Tahir, Z., Mahmood, S. A., & Tariq, A. (2025). Analyzing and predicting land use and land cover dynamics using multispectral high-resolution imagery and hybrid CA-Markov modeling. *Land Use Policy*, *157*, 107655. https://doi.org/10.1016/j.landusepol.2025.107655

Dudeen, B. (2013). *The Soils of Palestine (The West Bank and Gaza Strip) Current Status and Future Perspectives*. https://www.semanticscholar.org/paper/The-Soils-of-Palestine-(The-West-Bank-and-Gaza-and-Dudeen/ea7008834b942fa390cfc3e69a6b3e4563950ed6

Eastman, J. R. (2024). *TerrSet Manual* [Manual]. Clark University.

Eastman, J. R., Labs, C., & University, C. (2024). *TerrSet Tutorial*.

Ergen, M. (2025). Spatıotemporal analysıs of urban development and land USE in sakarya provınce, Türkiye: Implıcatıons for future urban growth modelıng. *GeoJournal*, *90*(3), 112. https://doi.org/10.1007/s10708-025-11363-z

Falah, N., Karimi, A., & Harandi, A. T. (2020). Urban growth modeling using cellular automata model and AHP (case study: Qazvin city). *Modeling Earth Systems and Environment*, *6*(1), 235–248. https://doi.org/10.1007/s40808-019-00674-z

Fattah, Md. A., Morshed, S. R., & Morshed, S. Y. (2021). Multi-layer perceptron-Markov chain-based artificial neural network for modelling future land-specific carbon emission pattern and its influences on surface temperature. *SN Applied Sciences*, *3*(3), 359. https://doi.org/10.1007/s42452-021-04351-8

Fontana, A. G., Nascimento, V. F., Ometto, J. P., & do Amaral, F. H. F. (2023). Analysis of past and future urban growth on a regional scale using remote sensing and machine learning. *Frontiers in Remote Sensing*, *4*. https://doi.org/10.3389/frsen.2023.1123254

Ghodieh, A. (2020). Urban Built-Up Area Estimation and Change Detection of the Occupied West Bank, Palestine, Using Multi-temporal Aerial Photographs and Satellite Images. *Journal of the Indian Society of Remote Sensing*, *48*(2), 235–247. https://doi.org/10.1007/s12524-019-01073-8

Girma, R., Fürst, C., & Moges, A. (2022). Land use land cover change modeling by integrating artificial neural network with cellular Automata-Markov chain model in Gidabo river basin, main Ethiopian rift. *Environmental Challenges*, *6*, 100419. https://doi.org/10.1016/j.envc.2021.100419

Gómez, J. A., Patiño, J. E., Duque, J. C., & Passos, S. (2019). Spatiotemporal Modeling of Urban Growth Using Machine Learning. *Remote Sensing*, *12*(1). https://doi.org/10.3390/rs12010109

Gupta, S. (2025). Integrating Machine Learning, Cellular Automata-Artificial Neural Network Model for Projecting Future Land Use Patterns in Urban Landscape of Jaipur, India. *Research in Ecology*, 32–51. https://doi.org/10.30564/re.v7i4.9819

Hanoon, S. K., Abdullah, A. F., Shafri, H. Z. M., & Wayayok, A. (2023). Urban Growth Forecast Using Machine Learning Algorithms and GIS-Based Novel Techniques: A Case Study Focusing on Nasiriyah City, Southern Iraq. *ISPRS International Journal of Geo-Information*, *12*(2), 76. https://doi.org/10.3390/ijgi12020076

Helal, A., & Zawawi, Z. (2024). Land Cover and Land Surface Temperature in the West Bank, Palestine. *Advances in Civil Engineering*, *2024*(1), 1107242. https://doi.org/10.1155/2024/1107242

Helu, M. F. A. (2012). Urban Sprawl in Palestinian Occupied Territories: Causes, Consequences and Future. *Environment and Urbanization ASIA*, *3*(1), 121–141. https://doi.org/10.1177/097542531200300107

Holail, S., Saleh, T., Xiao, X., Xiao, J., Xia, G.-S., Shao, Z., Wang, M., Gong, J., & Li, D. (2024). Time-series satellite remote sensing reveals gradually increasing war damage in the Gaza Strip. *National Science Review*, *11*(9), nwae304. https://doi.org/10.1093/nsr/nwae304

Kasraian, D., Maat, K., & van Wee, B. (2019). The impact of urban proximity, transport accessibility and policy on urban growth: A longitudinal analysis over five decades. *Environment and Planning B: Urban Analytics and City Science*, *46*(6), 1000–1017. https://doi.org/10.1177/2399808317740355

Khajuria, N., & Kaushik, S. P. (2024). Dynamic trends in land surface temperature and land use/land cover transitions in semi-arid metropolitan city, Jaipur. *Environmental Monitoring and Assessment*, *197*(1), 47. https://doi.org/10.1007/s10661-024-13370-y

Kraft, D. (2009, June 3). How a Settlement's 'Natural Growth' Appears at Ground Level. *Jewish Journal*. https://jewishjournal.com/israel/70691/

Kuhail, S., & Radwan, A. M. (2025). Satellite Imagery Analysis of The Gaza Strip Using Remote Sensing and Machine Learning Techniques | Request PDF. *Israa University Journal for Applied Science*. https://doi.org/10.52865/XSMX3932

Lovelace, R., Nowosad, J., & Muenchow, J. (2019). *Chapter 15 Ecology | Geocomputation with R*. https://r.geocompx.org/eco.html

Mehra, N., & Swain, J. B. (2023). Use of enhanced vegetation index (EVI) as a land cover classification tool and its suitability in urban development studies. *AIP Conference Proceedings*, *2852*(1), 130004. https://doi.org/10.1063/5.0164422

Ministry of Agriculture. (2016). *West Bank Land Use/Land Cover Map* [Dataset]. G.I.S Dep.

Modi'in Illit (West Bank) | The National Library of Israel. (n.d.). Retrieved January 10, 2026, from https://www.nli.org.il/en/a-topic/987007467975005171

Moghayer, T. J. T., Daget, Y. T., & Wang, X. (2017). Challenges of urban planning in Palestine. *IOP Conference Series: Earth and Environmental Science*, *81*(1), 012152. https://doi.org/10.1088/1755-1315/81/1/012152

Muhsen, M. (2017). *Urban Transformations in the West Bank of Palestine, Drivers and Consequences: A case of Ramallah Area*.

Mustak, S., Baghmar, N. K., Singh, S. K., & Srivastava, P. K. (2022). Multi-scenario based urban growth modeling and prediction using earth observation datasets towards urban policy improvement. *Geocarto International*, *37*(27), 18275–18303. https://doi.org/10.1080/10106049.2022.2138983

Nassar, M., Levy, R., Keough, N., & Nassar, N. N. (2019). Agricultural Land Use Change and its Drivers in the Palestinian Landscape Under Political Instability, the Case of Tulkarm City. *Journal of Borderlands Studies*, *34*(3), 377–394. https://doi.org/10.1080/08865655.2017.1344561

Nazer, S., Abughannam ,Rana, & and Khasib, S. (2019). Landscape change in Ramallah—Palestine (1994–2014). *Landscape Research*, *44*(5), 541–556. https://doi.org/10.1080/01426397.2018.1495184

Nikoo, M. R., Zarei, E., & Al-Wardy, M. (2025). Mapping coastal transformations with a novel Cellular Automata–Markov–Random forest framework for land use change modeling. *Scientific Reports*, *16*(1), 1469. https://doi.org/10.1038/s41598-025-31791-8

Ofran, H., & Shem-Tov, A. (2017). *Unraveling the Mechanism behind Illegal Outposts* (Settlement Watch). PeaceNow. https://peacenow.org.il/wp-content/uploads/2017/03/unraveling-the-mechanism-behind-illegal-outpots-full-report-1.pdf

Peace Now. (2024). *GIS Layers of Settlements*. https://peacenow.org.il/en/gis-layers-peace-now-maps

Peace Now. (2025). *Settlements and Outposts Peace Now 12.2025* [Spreadsheet]. https://docs.google.com/spreadsheets/d/1Hs_JdYPEs4oXs09zG3Hd4tWBpYo0ImkJ6WuXAEgMi0U/edit

Peace Now Who We Are. (n.d.). Retrieved February 6, 2026, from https://peacenow.org.il/en/about-us/who-are-we

Pimple, U., Simonetti, D., Sitthi, A., Pungkul, S., Leadprathom, K., Skupek, H., Som-ard, J., Gond, V., & Towprayoon, S. (2017). Google Earth Engine Based Three Decadal Landsat Imagery Analysis for Mapping of Mangrove Forests and Its Surroundings in the Trat Province of Thailand. *Journal of Computer and Communications*, *6*(1), 247–264. https://doi.org/10.4236/jcc.2018.61025

Pontius Jr, R. G., Francis, T., & Millones, M. (2025). A call to interpret disagreement components during classification assessment. *International Journal of Geographical Information Science*, *39*(7), 1373–1390. https://doi.org/10.1080/13658816.2025.2469830

Pontius Jr, R. G., & Millones, M. (2011). Death to Kappa: Birth of quantity disagreement and allocation disagreement for accuracy assessment. *International Journal of Remote Sensing*, *32*(15), 4407–4429. https://doi.org/10.1080/01431161.2011.552923

Pontius, R. G. (2002). Statistical methods to partition effects of quantity and location during comparison of categorical maps at multiple resolutions. *Photogrammetric Engineering and Remote Sensing*, *68*(10), 1041–1049.

Probst, P., Wright, M. N., & Boulesteix, A.-L. (2019). Hyperparameters and tuning strategies for random forest. *WIREs Data Mining and Knowledge Discovery*, *9*(3), e1301. https://doi.org/10.1002/widm.1301

Qian, J., Zhou, Q., Chen, X., & Sun, B. (2020). A Model-Based Analysis of Spatio-Temporal Changes of the Urban Expansion in Arid Area of Western China: A Case Study in North Xinjiang Economic Zone. *Atmosphere*, *11*(9). https://doi.org/10.3390/atmos11090989

Rahimi, E., & Jung, C. (2024). Evaluating the applicability of landsat 8 data for global time series analysis. *Frontiers in Remote Sensing*, *5*. https://doi.org/10.3389/frsen.2024.1492534

Rasul, A., Balzter, H., Ibrahim, G. R. F., Hameed, H. M., Wheeler, J., Adamu, B., Ibrahim, S., & Najmaddin, P. M. (2018). Applying Built-Up and Bare-Soil Indices from Landsat 8 to Cities in Dry Climates. *Land*, *7*(3), 81. https://doi.org/10.3390/land7030081

Rimal, B., Sloan, S., Keshtkar, H., Sharma, R., Rijal, S., & Shrestha, U. B. (2020). Patterns of Historical and Future Urban Expansion in Nepal. *Remote Sensing*, *12*(4). https://doi.org/10.3390/rs12040628

Sbaih, L. R., & Thawaba, S. (2025). Geopolitics Implication on Urban Growth: Case Studies from Palestine. *Journal of Borderlands Studies*, *0*(0), 1–21. https://doi.org/10.1080/08865655.2025.2565555

Schwake, G. (2020). The Privatisation of a National Project: The settlements along the Trans-Israel Highway since 1977. *A+BE | Architecture and the Built Environment*, (14), 1–416.

Selmy, S. A. H., Kucher, D. E., Mozgeris, G., Moursy, A. R. A., Jimenez-Ballesta, R., Kucher, O. D., Fadl, M. E., & Mustafa, A. A. (2023). Detecting, Analyzing, and Predicting Land Use/Land Cover (LULC) Changes in Arid Regions Using Landsat Images, CA-Markov Hybrid Model, and GIS Techniques. *Remote Sensing*, *15*(23). https://doi.org/10.3390/rs15235522

Singer, J. (2021). West Bank Areas A, B and C – How Did They Come into Being? *International Negotiation*, *26*(3), 391–401. https://doi.org/10.1163/15718069-bja10030

Singh, B., Venkatramanan, V., & Deshmukh, B. (2022). Monitoring of land use land cover dynamics and prediction of urban growth using Land Change Modeler in Delhi and its environs, India. *Environmental Science and Pollution Research*, *29*(47), 71534–71554. https://doi.org/10.1007/s11356-022-20900-z

Sisay, G., Gessesse, B., Fürst, C., Kassie, M., & Kebede, B. (2023). Modeling of land use/land cover dynamics using artificial neural network and cellular automata Markov chain algorithms in Goang watershed, Ethiopia. *Heliyon*, *9*(9), e20088. https://doi.org/10.1016/j.heliyon.2023.e20088

Sonet, M. S., Hasan, Md. Y., Kafy, A. A., & Shobnom, N. (2025). Spatiotemporal analysis of urban expansion, land use dynamics, and thermal characteristics in a rapidly growing megacity using remote sensing and machine learning

techniques. *Theoretical and Applied Climatology*, *156*(2), 79. https://doi.org/10.1007/s00704-024-05264-3

Souza, E. M. F. da R. de, Gomes, A. A. T., & Viegas, V. S. (2025). *Urban Growth in Metropolitan Regions Using Dynamic Modeling by Cellular Automata: A Comparative Analysis Between Brazil and Portuga*. Proceedings of the 11th International Conference on Geographical Information Systems Theory, Applications and Management. https://doi.org/10.5220/0013205000003935

Spyer, J. (2006). Israel's Disengagement Plan: Conception and Implementation. *IEMed*. https://www.iemed.org/publication/israels-disengagement-plan-conception-and-implementation/

Tahmi, S., Rui, X., & Guechi, I. (2025). Modeling and evaluation of urban growth: A comparative approach between XGBoost and deep neural networks coupled with multi-criteria analysis: case of BouSaâda, Algeria. *Modeling Earth Systems and Environment*, *12*(1), 37. https://doi.org/10.1007/s40808-025-02658-8

Tang, X., Liu, F., & Hu, X. (2024). Urban growth simulation and scenario projection for the arid regions using heuristic cellular automata. *Scientific Reports*, *14*(1), 21106. https://doi.org/10.1038/s41598-024-71709-4

Tariq, A., Yan, J., & Mumtaz, F. (2022). Land change modeler and CA-Markov chain analysis for land use land cover change using satellite data of Peshawar, Pakistan. *Physics and Chemistry of the Earth, Parts A/B/C*, *128*, 103286. https://doi.org/10.1016/j.pce.2022.103286

Tenenbaum, K., & Eiran, E. (2005). Israeli Settlement Activity in the West Bank and Gaza: A Brief History. *Negotiation Journal*, *21*(2), 171–175. https://doi.org/10.1111/j.1571-9979.2005.00055.x

The Applied Research Institute – Jerusalem. (2008, May 5). While debating about settlements; “Israel declared the settlement of Modi’in 'Illit as the third Jewish city in the occupied West Bank.” *POICA*. https://poica.org/2008/05/while-debating-about-settlements-israel-declared-the-settlement-of-modiin-illit-as-the-third-jewish-city-in-the-occupied-west-bank/

Torchiana, A. L., Rosenbaum, T., Scott, P. T., & Souza-Rodrigues, E. (2025). Improving Estimates of Transitions from Satellite Data: A Hidden Markov Model Approach. *The Review of Economics and Statistics*, *107*(2), 426–441. https://doi.org/10.1162/rest_a_01301

UNHRC. (2013). *Report of the independent international factfinding mission to investigate the implications of the Israeli settlements on the civil, political, economic, social and cultural rights of the Palestinian people throughout the Occupied Palestinian Territory, including East Jerusalem* (Human Rights Situation in Palestine and Other Occupied Arab Territories). United Nations Human Rights Council. https://docs.un.org/en/A/HRC/22/63

UNHRC. (2025, August 14). Report of the Independent International Commission of Inquiry (A/80/337) examining land and housing in the Occupied Palestinian Territory and in Israel and presents a summary of the Commission’s findings on the crime of genocide. *Question of Palestine*. https://www.un.org/unispal/document/report-of-coi-14aug25/

United Nations. (2023, March 28). Human Rights Council Hears that 700,000 Israeli Settlers are Living Illegally in the Occupied West Bank—Meeting Summary (Excerpts). *Question of Palestine*. https://www.un.org/unispal/document/human-rights-council-hears-that-700000-

israeli-settlers-are-living-illegally-in-the-occupied-west-bank-meeting-summary-excerpts/

UNRWA. (2025). *2024 Report on Israeli settlements in the occupied West Bank, including East Jerusalem Reporting period -January—December 2024*. European Union. https://www.eeas.europa.eu/sites/default/files/2025/documents/Report%20on%20Israeli%20Settlements%20in%20the%20occupied%20West%20Bank%20including%20East%20Jerusalem%20%28Reporting%20period%20January%20-%20December%202024%29.pdf

UNTERM. (2013). Green Line. In *United Nations Department for General Assembly and Conference Management*. United Nations. https://unterm.un.org/unterm2/en/view/dae03e47-c23e-4621-8761-a54c45459fd3

Varga, O. G., Pontius, R. G., Singh, S. K., & Szabó, S. (2019). Intensity Analysis and the Figure of Merit's components for assessment of a Cellular Automata – Markov simulation model. *Ecological Indicators*, *101*, 933–942. https://doi.org/10.1016/j.ecolind.2019.01.057

Vinayak, B., Lee, H. S., & Gedem, S. (2021). Prediction of Land Use and Land Cover Changes in Mumbai City, India, Using Remote Sensing Data and a Multilayer Perceptron Neural Network-Based Markov Chain Model. *Sustainability*, *13*(2). https://doi.org/10.3390/su13020471

Yang, C., & Zhao, S. (2022). Urban vertical profiles of three most urbanized Chinese cities and the spatial coupling with horizontal urban expansion. *Land Use Policy*, *113*, 105919. https://doi.org/10.1016/j.landusepol.2021.105919

Yatoo, S. A., Sahu, P., Kalubarme, M. H., & Kansara, B. B. (2022). Monitoring land use changes and its future prospects using cellular automata simulation and artificial neural network for Ahmedabad city, India. *GeoJournal*, *87*(2), 765–786. https://doi.org/10.1007/s10708-020-10274-5

Zerbini, A., & Fradley, M. (2018). Higher Resolution Satellite Imagery of Israel and Palestine: Reassessing the Kyl-Bingaman Amendment. *Space Policy*, *44–45*, 14–28. https://doi.org/10.1016/j.spacepol.2018.03.002

Zhang, A., Tariq, A., Quddoos, A., Naz, I., Aslam, R. W., Barboza, E., Ullah, S., & Abdullah-Al-Wadud, M. (2025). Spatio-temporal analysis of urban expansion and land use dynamics using google earth engine and predictive models. *Scientific Reports*, *15*(1), 6993. https://doi.org/10.1038/s41598-025-92034-4

Zhang, X., Zhao, T., Xu, H., Liu, W., Wang, J., Chen, X., & Liu, L. (2024). GLC_FCS30D: The first global 30 m land-cover dynamics monitoring product with a fine classification system for the period from 1985 to 2022 generated using dense-time-series Landsat imagery and the continuous change-detection method. *Earth System Science Data*, *16*(3), 1353–1381. https://doi.org/10.5194/essd-16-1353-2024

Zhang, Y., & Zhao, H. (2020). Land–Use and Land-Cover Change Detection Using Dynamic Time Warping–Based Time Series Clustering Method. *Canadian Journal of Remote Sensing*, *46*(1), 67–83. https://doi.org/10.1080/07038992.2020.1740083

APPENDIX

A) LITERATURE REVIEW

Link

B) TABLE OF BAND INDICES/PERMUTATION

1994

variable	MeanDecreaseAccuracy
blue	0.104182
veg_NDVImean_variance	0.078839
NDVI_mean	0.07498
green	0.073985
red	0.059823
NDVI_monthly_var	0.057604
NDMI_mean	0.05484
built_SWIR_variance	0.052106
nir	0.050757
dbsi	0.047336
mndwi	0.047105
swir	0.030702
SAVI_mean	0.030488
mndbi	0.02621
NBR_var	0.025311
swir2	0.02466
NDVI_var	0.023568
SAVI_var	0.023128
veg_NDVImean_contrast	0.022688
veg_NDVImean_entropy	0.020231
NDVI_amp	0.016632
EVI_mean	0.012694
NDMI_var	0.012605
EVI_var	0.01119
NDVI_CV	0.010998
NBR_mean	0.010577
built_SWIR_contrast	0.006696
built_SWIR_dissimilarity	0.006471
built_SWIR_entropy	0.00162
veg_NDVImean_homogeneity	-4.9E-06

2014

variable	MeanDecreaseAccuracy
veg_veg_NDVImean_variance	0.122895
built_SWIR_variance	0.099097

mndwi	0.073262
NDVI_mean	0.065665
NDMI_mean	0.059363
NBR_var	0.05412
NDVI_monthly_var	0.051993
nir	0.048347
swir	0.042529
dbsi	0.036357
SAVI_mean	0.035667
red	0.029404
NDVI_amp	0.027976
NDVI_var	0.02634
green	0.02617
mndbi	0.025881
SAVI_var	0.025777
EVI_var	0.02502
blue	0.02402
EVI_mean	0.021276
NDMI_var	0.020282
swir2	0.019694
NDVI_CV	0.01584
NBR_mean	0.012993
veg_veg_NDVImean_contrast	0.012331
veg_veg_NDVImean_entropy	0.011346
built_SWIR_contrast	0.00772
built_SWIR_entropy	0.004671
built_SWIR_dissimilarity	0.002051
veg_veg_NDVImean_homogeneity	2.77E-05

2024

variable	**MeanDecreaseAccuracy**
built_SWIR_variance	0.087025
veg_NDVImean_variance	0.077779
NDVI_mean	0.064035
SAVI_mean	0.049901
NDVI_monthly_var	0.048721
NBR_var	0.048458
mndwi	0.044315
swir	0.041875
nir	0.039596
NDVI_var	0.037141
NDMI_var	0.036283
swir2	0.035619
dbsi	0.035173
EVI_mean	0.035018
green	0.032942
SAVI_var	0.032816
red	0.032437

EVI_var	0.029799
veg_NDVImean_entropy	0.029314
veg_NDVImean_contrast	0.026857
blue	0.026404
NDMI_mean	0.025867
mndbi	0.025434
NDVI_CV	0.018841
NDVI_amp	0.018298
NBR_mean	0.018226
built_SWIR_contrast	0.008717
built_SWIR_entropy	0.004546
built_SWIR_dissimilarity	0.001119
veg_NDVImean_homogeneity	0.000518

C) CLASS BALANCE AND LOCATIONS FOR RF

1994

landcover	landcover_name	train_n	test_n	total_n
1	Agriculture	282	121	403
2	Bare	249	108	357
3	Forest	247	106	353
4	Built	270	117	387

2014

landcover	landcover_name	train_n	test_n	total_n
1	Agriculture	269	116	385
2	Bare	289	125	414
3	Forest	269	116	385
4	Built	298	128	426

2024

landcover	landcover_name	train_n	test_n	total_n
1	Agriculture	269	116	385
2	Bare	264	114	378
3	Forest	275	118	393
4	Built	304	131	435

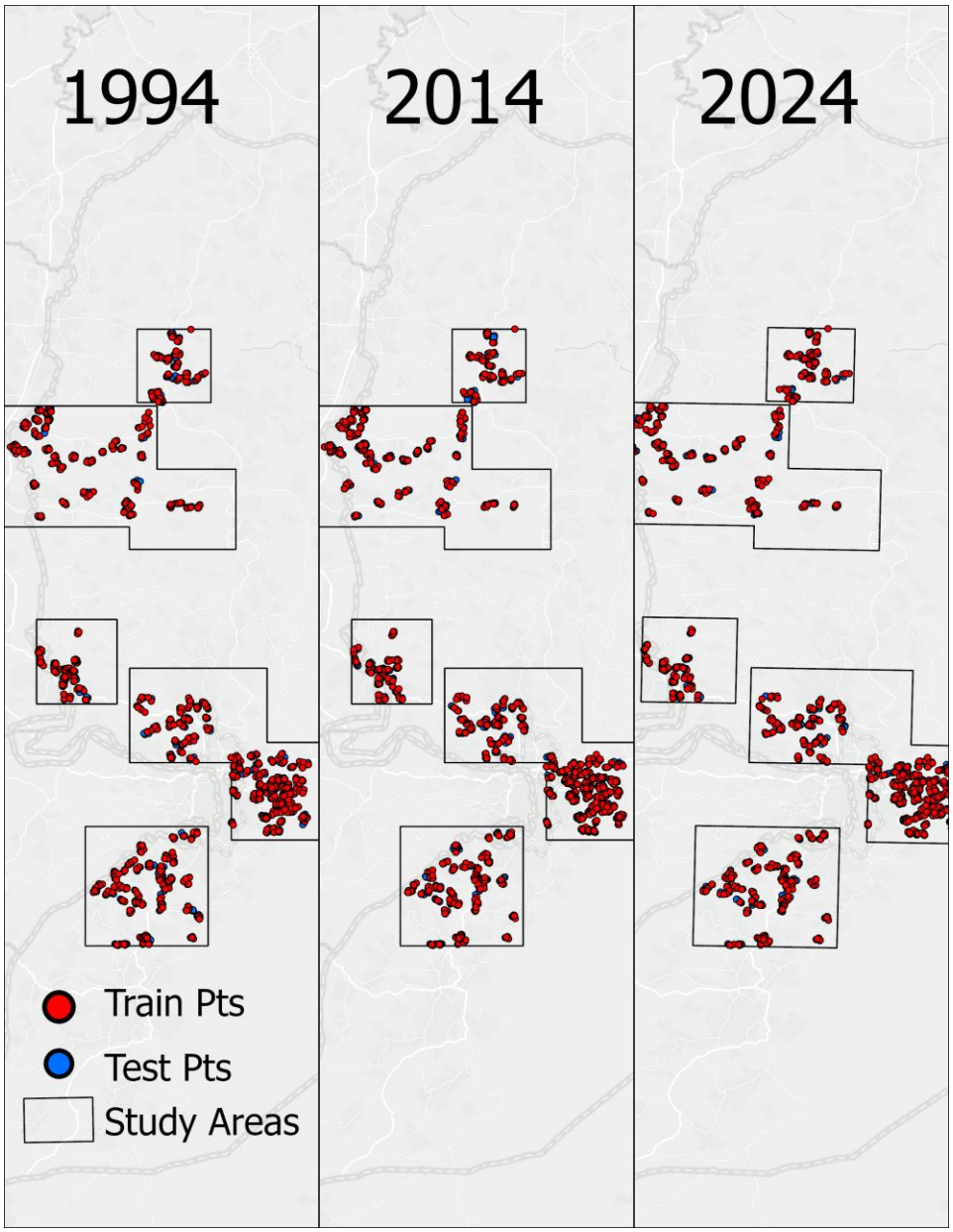

D) MLP MODEL RESULTS

Variable	bare	farm	vegetation
Hidden nodes		4	
Iterations before stop		10,000	
Sample size	5,219	8,430	3,485
OOB Accuracy	95.12	89.46	90.27
OOB Skill	0.80	0.79	0.80

E) DRIVER SOURCES

Driver	Source
Barriers (Areas A+B and Separation Wall)	Ofran, H. (2024). Peace_Now_Layers [Dataset]. ArcGIS Online. https://www.arcgis.com/home/item.html?id=e3848dc0a04c44cc9ad9f7db228cd3a3
Cities	OpenStreetMap contributors. (2014). Israel and Palestine [Dataset]. Geofabrik.de. https://download.geofabrik.de/asia.html#
Elevation	ASA Jet Propulsion Laboratory (JPL). (2013). NASA Shuttle Radar Topography Mission Global 1 arc second V003 [Dataset]. NASA EOSDIS Land Processes Distributed Active Archive Center (LP DAAC). https://doi.org/10.5067/MEaSUREs/SRTM/SRTMGL1.003
Railways	OpenStreetMap contributors. (2014). Israel and Palestine [Dataset]. Geofabrik.de. https://download.geofabrik.de/asia.html#
Roads	OpenStreetMap contributors. (2014). Israel and Palestine [Dataset]. Geofabrik.de. https://download.geofabrik.de/asia.html#
1994 Settlement Area	Generated from the results of this research.
Slope	ASA Jet Propulsion Laboratory (JPL). (2013). NASA Shuttle Radar Topography Mission Global 1 arc second V003 [Dataset]. NASA EOSDIS Land Processes Distributed Active Archive Center (LP DAAC). https://doi.org/10.5067/MEaSUREs/SRTM/SRTMGL1.003
Towns	OpenStreetMap contributors. (2014). Israel and Palestine [Dataset]. Geofabrik.de. https://download.geofabrik.de/asia.html#
Waterways	OpenStreetMap contributors. (2014). Israel and Palestine [Dataset]. Geofabrik.de. https://download.geofabrik.de/asia.html#

F) RF CONFUSION MATRIX BEFORE TEMPORAL FILTERING

		Years		
	Variables	**1994**	**2014**	**2024**
Producer Accuracy	*Agriculture*	94.21	92.24	90.52
	Bare	94.44	98.40	95.61
	Vegetation	82.08	71.55	77.12
	Built	89.74	94.53	90.08
User Accuracy	*Agriculture*	80.85	83.59	81.40
	Bare	91.07	92.48	90.08
	Vegetation	95.60	90.22	92.86
	Built	97.22	91.67	90.08
Kappa Coefficient		0.87	0.87	0.84
Overall Accuracy		90.3	90.3	88.3

E) AREA COMPARISON OF GLC AND RF LULC RESULTS

	Year					
LULC	**1995**	**1994**	**2014**	**2014**	**2022**	**2024**
	GLC	**RF**	**GLC**	**RF**	**GLC**	**RF**
farm	75,485	68,852	62,132	57,269	61,937	49,596
bare	2,517	14,511	1,857	17,402	1,842	16,935
vegetation	23,431	13,886	22,724	16,035	22,346	20,376

built	4,557	9,940	19,275	16,454	19,818	20,282

Masters Program in **Geospatial Technologies**

Supported by:
Education and Culture
ERASMUS MUNDUS